

Supporting information

Could dissecting the molecular framework of β -lactam integrin ligands enhance selectivity?

Giulia Martelli, Monica Baiula, Alberto Caligiana, Paola Galletti, Luca Gentilucci, Roberto Artali, Santi Spampinato,* Daria Giacomini, *

List of contents:

- S2** Pharmacology
- S2** Cell culture
- S2** Cell adhesion assays
- S3** Competitive Solid-Phase Binding Assay
- S3** Scintillation Proximity-Binding Assay (SPA)
- S3** Western blot analysis
- S4** Molecular Modelling
- S6** Figure S3.
- S7** HLPC analyses
- S12** References
- S14** ^1H and ^{13}C spectra of compounds **2-12, 14, 16, 18-20, 22-25**.

Pharmacology

Cell culture. Jurkat E6.1 human T cells, Saos-2 and K562 cells were grown in RPMI-1640 (Life Technologies, Carlsbad, CA, USA) supplemented with L-glutamine and 10% FBS (fetal bovine serum; Life technologies). 40 h prior to experiments, K562 cells were incubated with 25 ng/mL PMA (Phorbol 12-myristate 13-acetate, Sigma-Aldrich SRL, Milan, Italy) to induce differentiation and to increase $\alpha_5\beta_1$ integrin expression. HEK293 cells were cultured in EMEM (Cambrex, Walkersville, MD, USA) with L-glutamine, nonessential aminoacids and 10% FBS. SK-MEL-24 cells were routinely grown in EMEM, supplemented with 10% FBS, nonessential aminoacids and sodium pyruvate. HEK293 cells were transfected with plasmids containing the coding sequence of α_v ¹ [a kind gift of Michael Davidson, Addgene plasmid no.57345] and β_3 subunit [a kind gift of Prof. S.J. Shattil] as previously reported². Cells were kept at 37 °C under 5% CO₂ humidified atmosphere. All cell lines were obtained from American Type Culture Collection (ATCC, Rockville, MD, USA). The cell lines employed are considered as useful *in vitro* models to investigate potential ligands that behave as agonists or antagonists of integrins.

Cell adhesion assays. The assays were performed as previously described^{2,3}. Briefly, for adhesion assay on Saos-2, SK-MEL-24 and K562 cells, 96-well plates (Corning Costar, Celbio, Milan, Italy) were coated by passive adsorption with fibronectin (10 µg/mL) overnight at 4 °C. After counting the cells, they were pre-incubated with various concentrations of each compound or with the vehicle (methanol) for 30 min at room temperature. Then 50000 cells/well were plated and incubated at room temperature for 1 h. Afterwards nonadherent cells were washed with 1% BSA (bovine serum albumin) in PBS (phosphate-buffered saline) and 50 µL of hexosaminidase substrate [4-nitrophenyl-N-acetyl-β-D-glucosaminide dissolved at a concentration of 7.5 mM in 0.09 M citrate buffer (pH 5) 0.5% Triton X-100 in H₂O] were added. After the addition of stopping solution [50 mM glycine and 5 mM EDTA (pH 10.4)] plates were read at 405 nm in an EnSpire Multimode Plate Reader (PerkinElmer, Waltham, MA, USA). For adhesion assays on Jurkat E6.1 cells, black 96-well plates were coated overnight at 4 °C with VCAM-1 (5 µg/mL) to study $\alpha_4\beta_1$ integrin-mediated adhesion. Jurkat E6.1 cells were stained with CellTracker green CMFDA (12.5 µM, 30 min at 37 °C, Life Technologies). After three washes, various concentrations of each compound or the vehicle (methanol) were added to Jurkat E6.1 cells for 30 min at 37 °C. Cells were then plated (500000/well) on VCAM-1 coated wells and incubated for 30 min at 37 °C. Three washes were performed to remove nonadherent cells and adhered cells were lysed with 0.5% Triton X-100 in PBS (30 min at 4 °C) and fluorescence was measured (Ex485 nm/Em535 nm). Experiments were carried out in quadruplicate and repeated at least three times. Data analysis and IC₅₀ or EC₅₀ values were calculated using GraphPad Prism 5.0 (GraphPad Software, San Diego, CA, USA). In another set of experiment, Jurkat E6.1 (500000 cells/well) or K562 or Saos-2 cells (50000 cells/well) were plated in 96-well plates previously coated directly with the most effective agonists under evaluation, dissolved in methanol to the final concentration of 10 µg/mL. Neutralizing antibodies towards α_4 (Santa Cruz Biotechnology) or α_v (Calbiochem, Merck) were pre-incubated 10 min with cells before plating on new compound coated wells. Adherent cell number was determined as previously described².

Competitive Solid-Phase Binding Assay. To determine integrin–ligand interactions, a solid-phase binding assay was employed using purified soluble integrins and coated fibronectin, as previously described². Briefly, black 96-well plates were coated with fibronectin 0.5 µg/mL in carbonate buffer (15 mM Na₂CO₃, 35 mM NaHCO₃, pH 9.6) overnight at 4 °C. Purified integrins (3 µg/mL for α_vβ₃; 10 µg/mL for α₅β₁) were incubated with the new compounds, employed at different concentrations (10⁻⁴ – 10⁻¹⁰ M) for 30 minutes, and then added into the coated wells for 1 h at room temperature. The plate was washed three times and primary antibody was added for 1 h at room temperature. Integrin antibodies were purchased from Calbiochem for α_v integrin (1:200) and BD Bioscience for α₅β₁ integrin (1:100). Then, secondary antibody AlexaFluor488 conjugated (1:400, ThermoFisher Scientific) was incubated after three washes for 1 h at room temperature. After washing three times, fluorescence was measured (Ex485 nm/Em535 nm). Experiments were carried out in triplicate and repeated at least three times. Data analysis and IC₅₀ values were calculated using GraphPad Prism 5.0.

Scintillation Proximity-Binding Assay (SPA). To evaluate α₄β₁ integrin-ligand interactions, we employed a SPA assay, as previously described^{2,4,5}. Briefly, 1 mg/50 mL antirabbit-coated beads (GE Healthcare Life Sciences), 200 mg of rabbit anti-α₄ integrin antibody (SantaCruz Biotechnology), and approximately 100 mg of purified α₄β₁ integrin were added in a scintillation vial. First, the α₄ integrin protein and the rabbit antihuman α₄ integrin antibody were incubated for 1 h at 4 °C; then the antirabbit antibody was added, and the three components were incubated for 2 h at 4 °C in the dark. [¹²⁵I]-FN was added to the vials and incubated overnight in constant agitation in the dark. The samples were read using a LS 6500 multipurpose scintillation counter (Beckham Coulter, Fullerton, CA, USA). Experiments were carried out in triplicate and repeated at least three times. Data analysis and IC₅₀ values were calculated using GraphPad Prism 5.0.

Western blot analysis. Cells were cultured for 16/18 h in medium containing 1% FBS. Then, 4 × 10⁶ cells were pre-incubated with different concentrations of the most effective de-structured compounds for 1 h and then seeded on VCAM-1- (2 µg/mL) or FN- (10 µg/mL) coated plates for 1 h. Cells were lysed using a mammalian protein extraction reagent (M-PER; Pierce, Rockford, IL, USA) in the presence of a phosphatase inhibitor cocktail. Protein extracts were quantified using a BCA protein assay kit (Pierce, Rockford, IL, USA), denatured for 5 min at 95°C, and separated by 12% SDS-PAGE gel. Proteins were subsequently transferred onto nitrocellulose membranes and immunoblotted with anti-phospho-ERK 1/2 or anti-total ERK1/2 antibodies (both 1:1000, Cell Signaling Technology, Danvers, MA, USA). After washing, membranes were incubated with anti-rabbit HRP-conjugated secondary antibodies (Santa Cruz Biotechnology, Dallas, TX, USA) for 1.5 h at room temperature. Image acquisition and analysis have been previously described⁶. Densitometric analysis of the bands is reported in Figure 2 (mean ± SEM; n=5); the amount of pERK1/2 is normalized to that of totERK1/2.

Molecular Modelling.

The structures were subjected to systematic conformer search followed by geometry optimization to the lowest energy structure with MOPAC7 (PM3, RMS gradient 0.01). The receptor models were obtained from the deposited X-ray structures: Protein Data Bank entry 4MMX for $\alpha v\beta 3$ integrin and 3VI4 for $\alpha 5\beta 1$ integrin. Hydrogen atoms were added with respect of hydrogen bonding network by Reduce software;⁷ PROPKA⁸ was employed to estimate the protonation states of the residues Asp, Glu, His, Lys, and Arg. Molecular docking experiments were performed with Autodock 4.0,⁹ using the Lamarckian Genetic Algorithm, which combines global (Genetic Algorithm alone) and local (Solis and Wets algorithm) search.¹⁰ Ligands and receptors were further processed using the Autodock Tool Kit (ADT).¹¹ Gasteiger-Marsili charges¹² were loaded on the ligands in ADT and solvation parameters were added to the final structure using the Addsol utility of Autodock. Each docking run consisted of an initial population of 100 randomly placed structures, maximum number of 200 energy evaluations, mutation rate 0.02, a crossover rate 0.80, elitism 1. For the local search, the so-called pseudo-Solis and Wets algorithm was applied using a maximum of 250 iterations per local search, for each ligand. The grid maps representing the system in the actual docking process were calculated with Autogrid. The dimensions of the grids were 100×100×100, with a spacing of 0.1 Å between the grid points and the centre close to the cavity left by the ligand after its removal. Docking results were scored by inter-molecular energy function based on the Weiner force field in Autodock. Results differing by less than 1.0 Å in positional root-mean-square deviation (rmsd) were clustered together and were represented by the result with the most favorable free energy of binding.

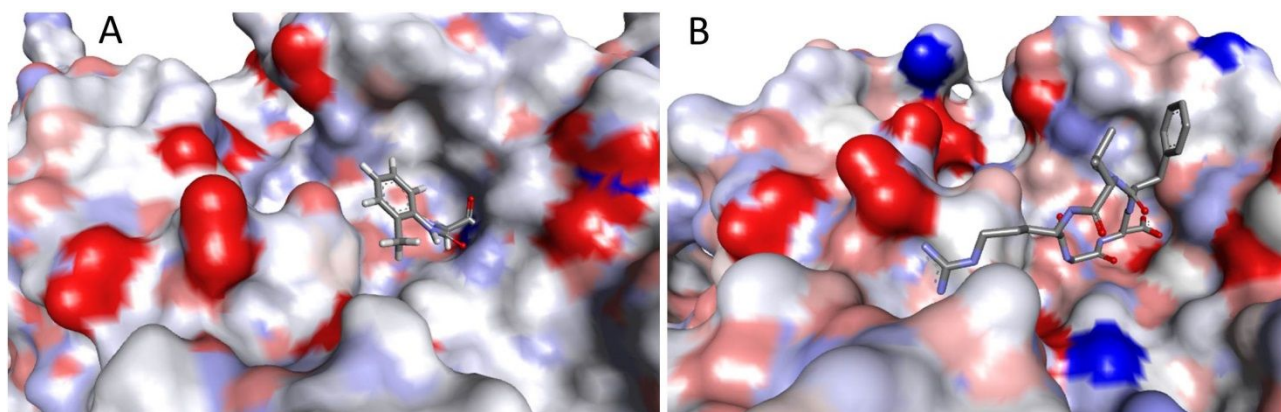


Figure S1. Comparison between the docked pose of compound **7** into the $\alpha v\beta 3$ integrin (pdb code: 4MMX) and the crystal structure of the complex cilengitide-extracellular segment of integrin $\alpha v\beta 3$ (pdb code: 1L5G).¹³ The ligand is rendered in sticks, the protein is represented by solid, closed water-accessible surface, colored by atom charge.

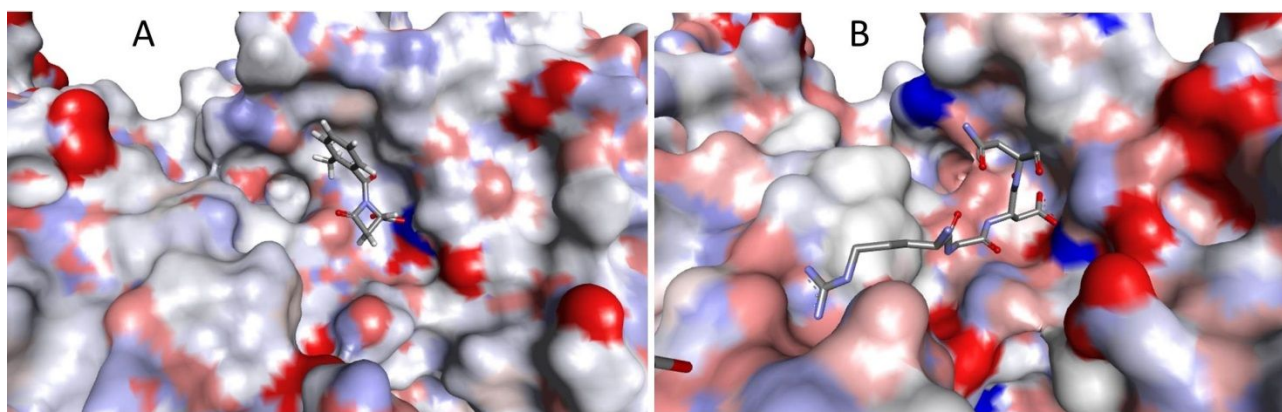


Figure S2. Comparison between the docked pose of compound **6** into the $\alpha_5\beta_1$ integrin (pdb code: 3VI4) and the crystal structure of the complex RGD tripeptide-integrin $\alpha_5\beta_1$ (pdb code: 3VI4). The ligand is rendered in sticks, the protein is represented by the solid, close water-accessible surface, colored by atom charge.

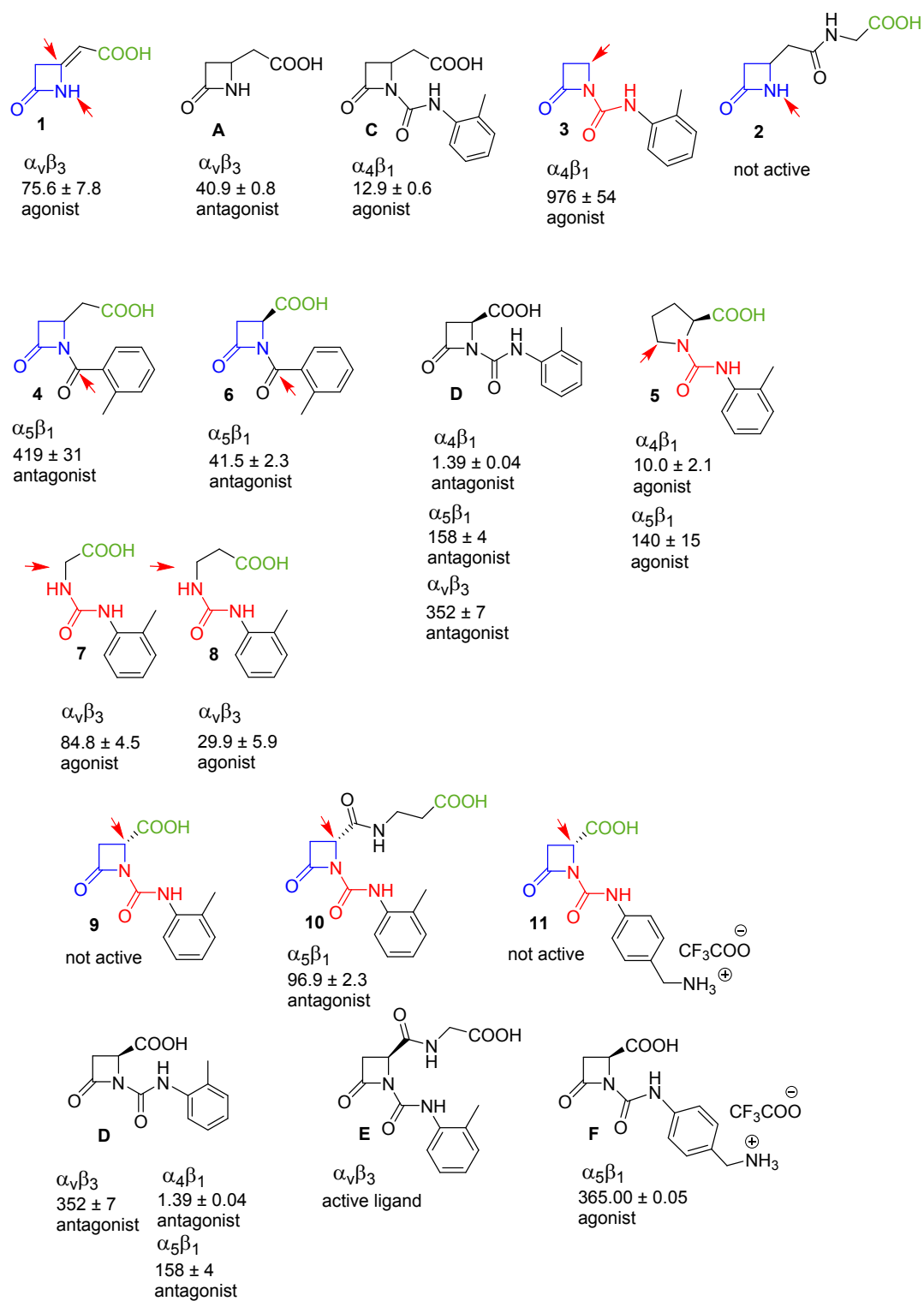
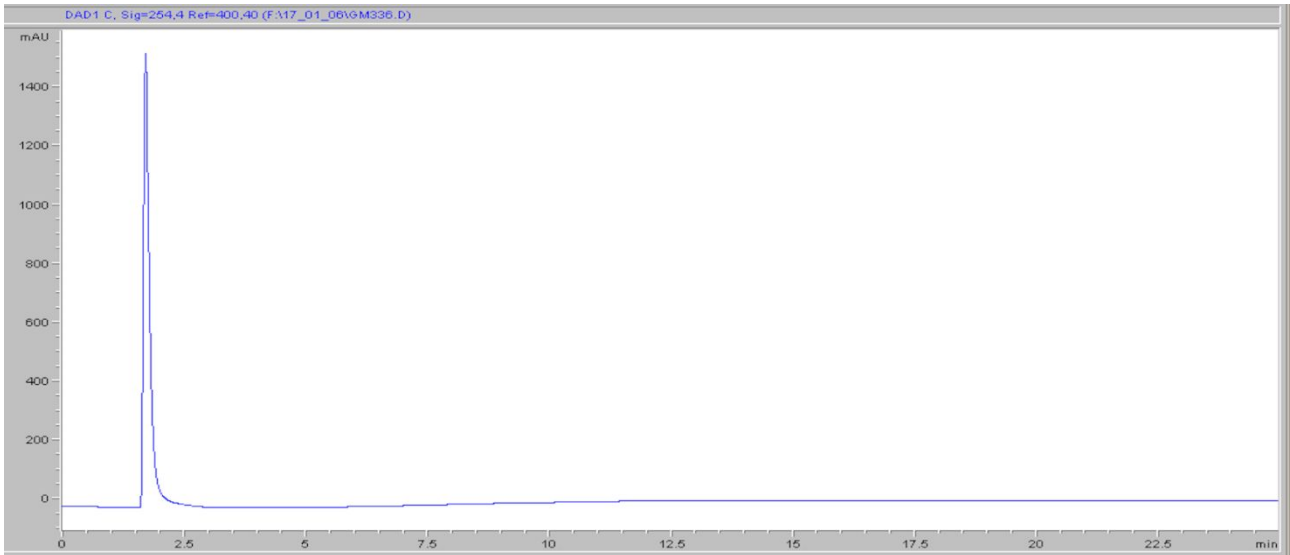


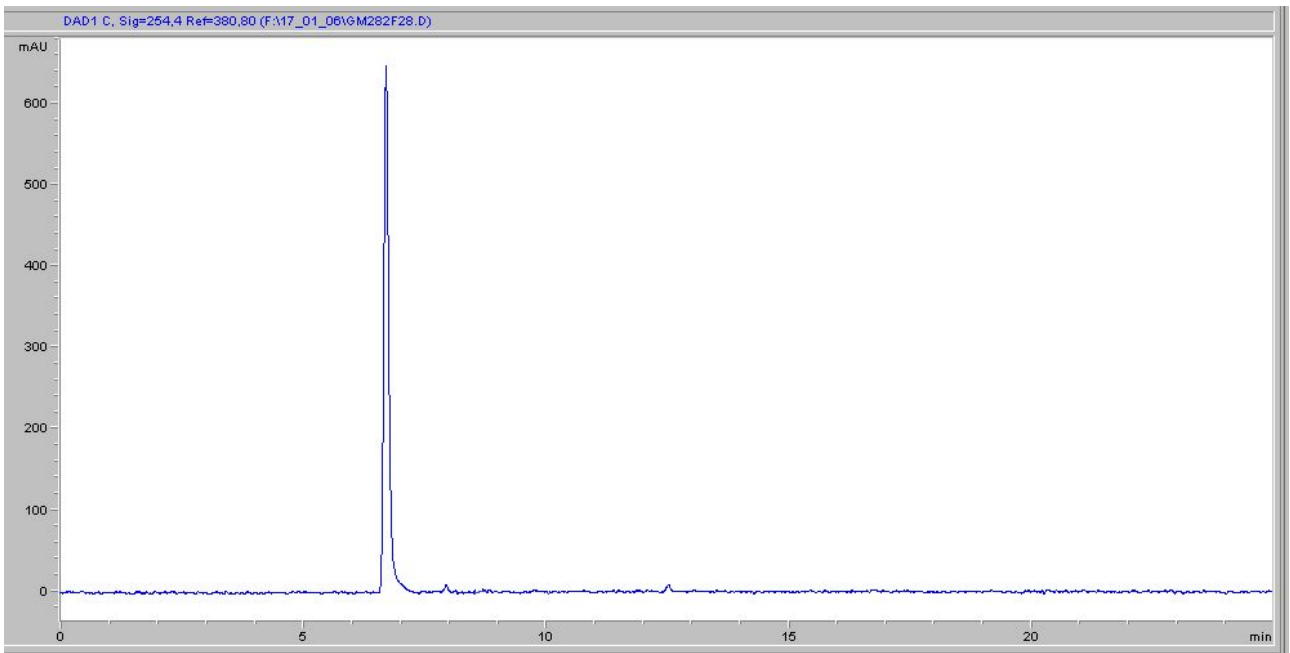
Figure S3. New compounds **1-11** and previously reported compounds **A-F** in comparison for the SAR discussion

HLPC analyses for purity

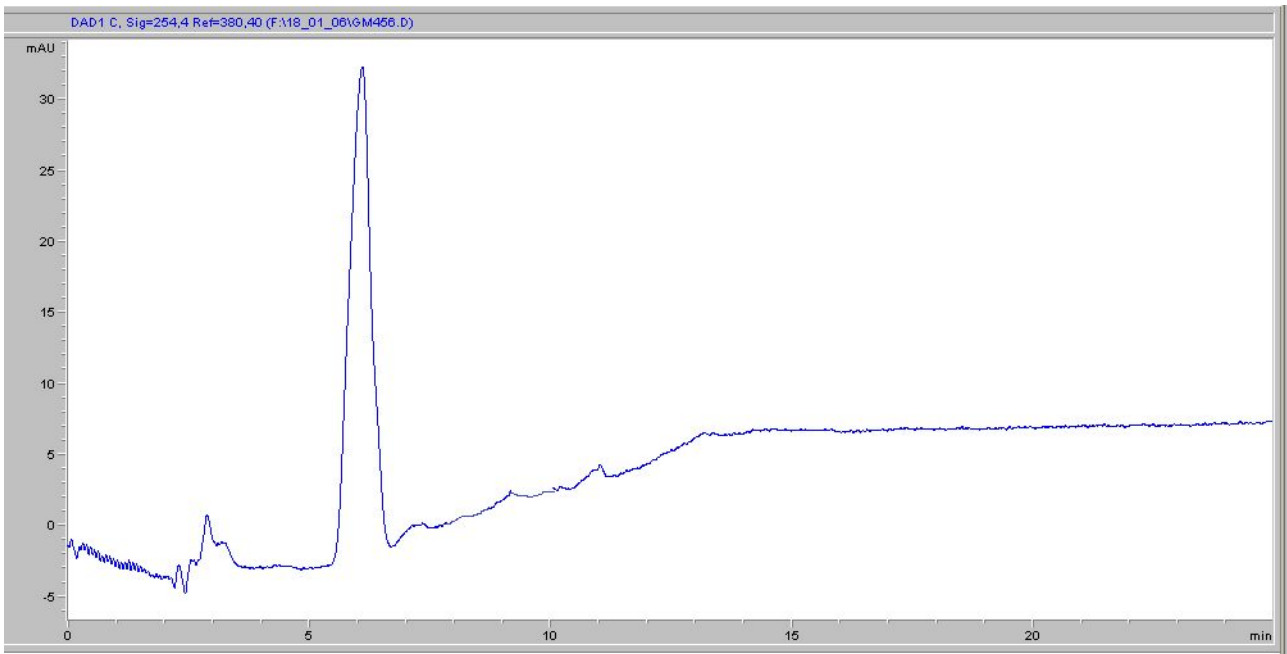
Compound 1



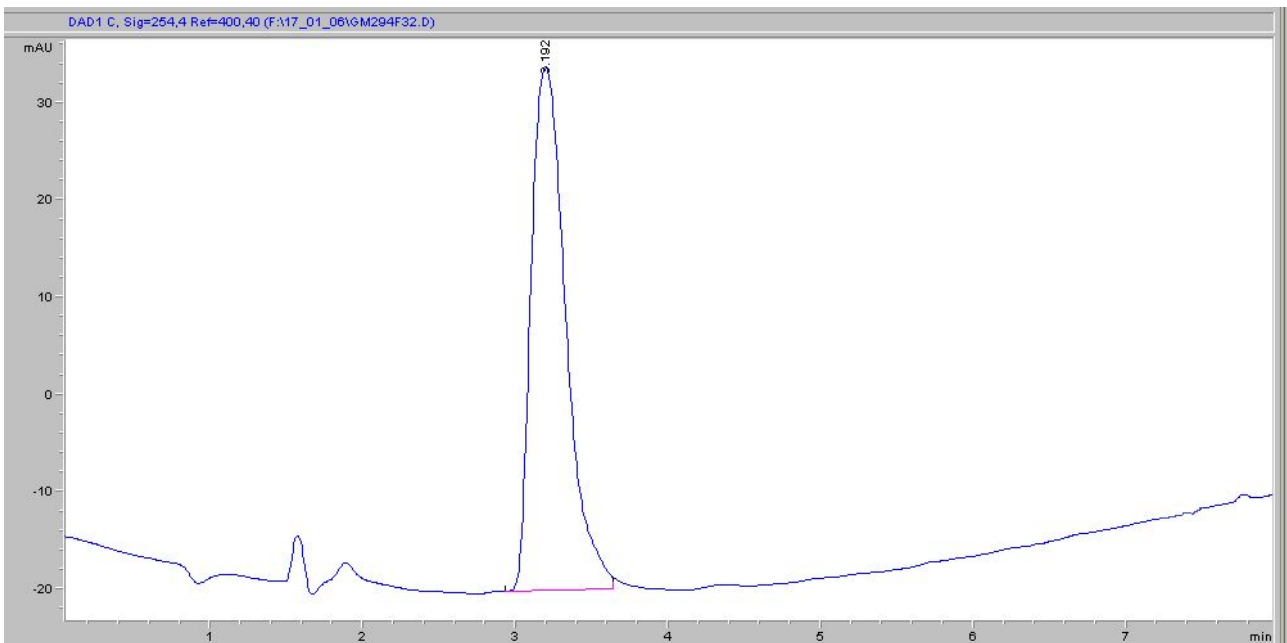
Compound 3



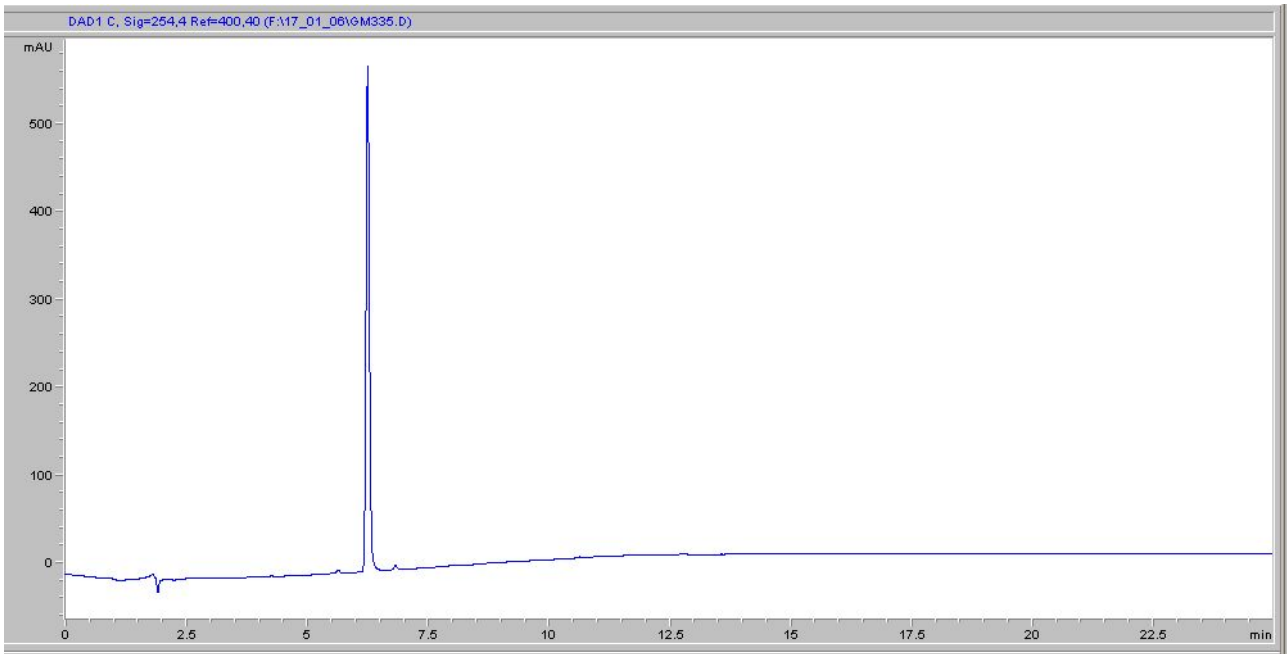
Compound 4



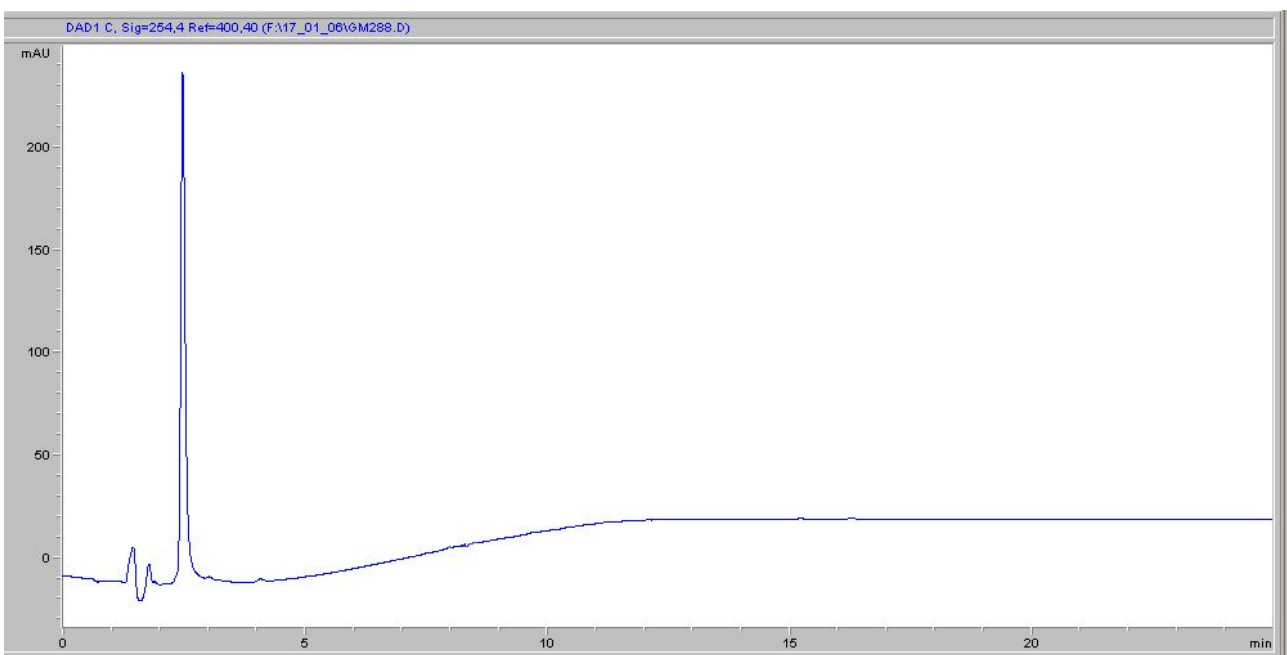
Compound 5



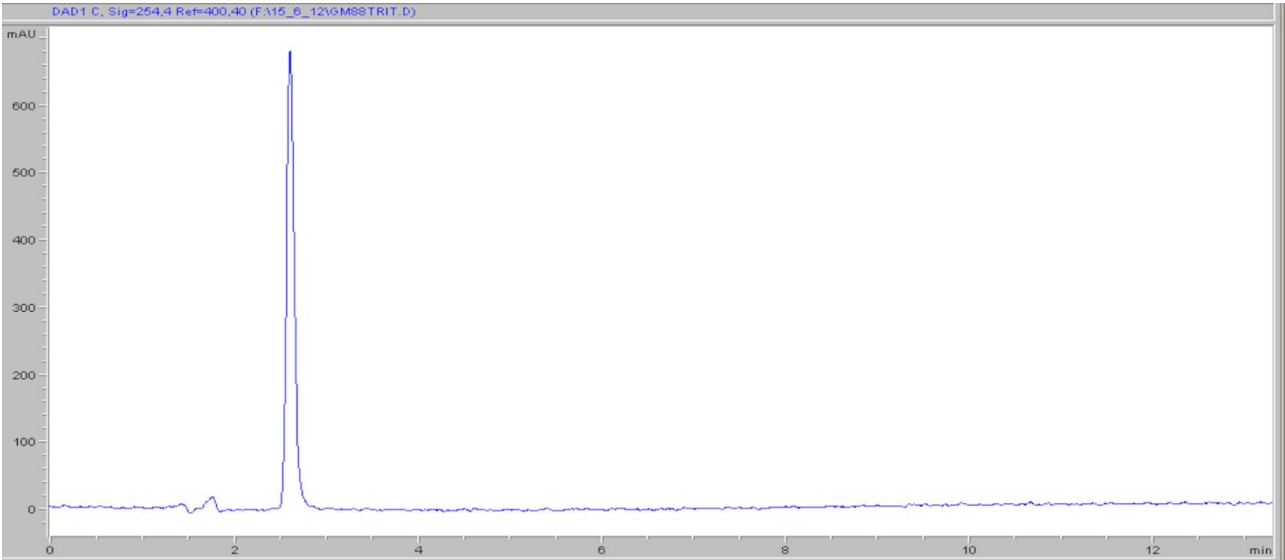
Compound 6



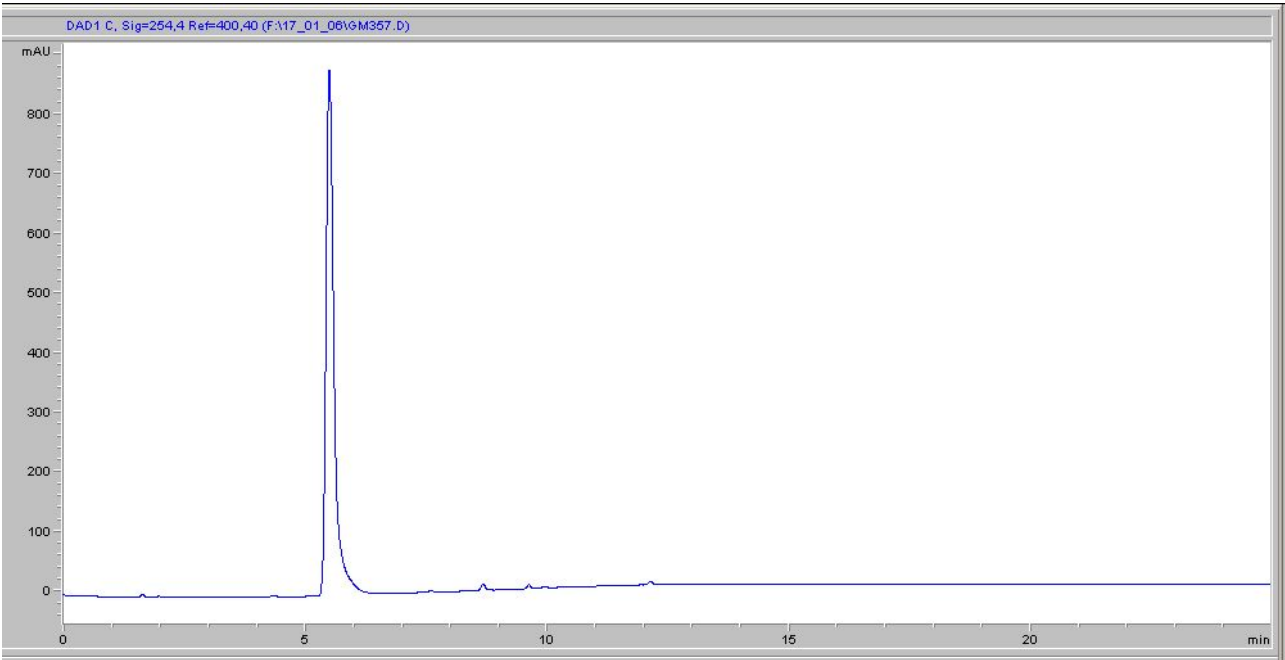
Compound 7



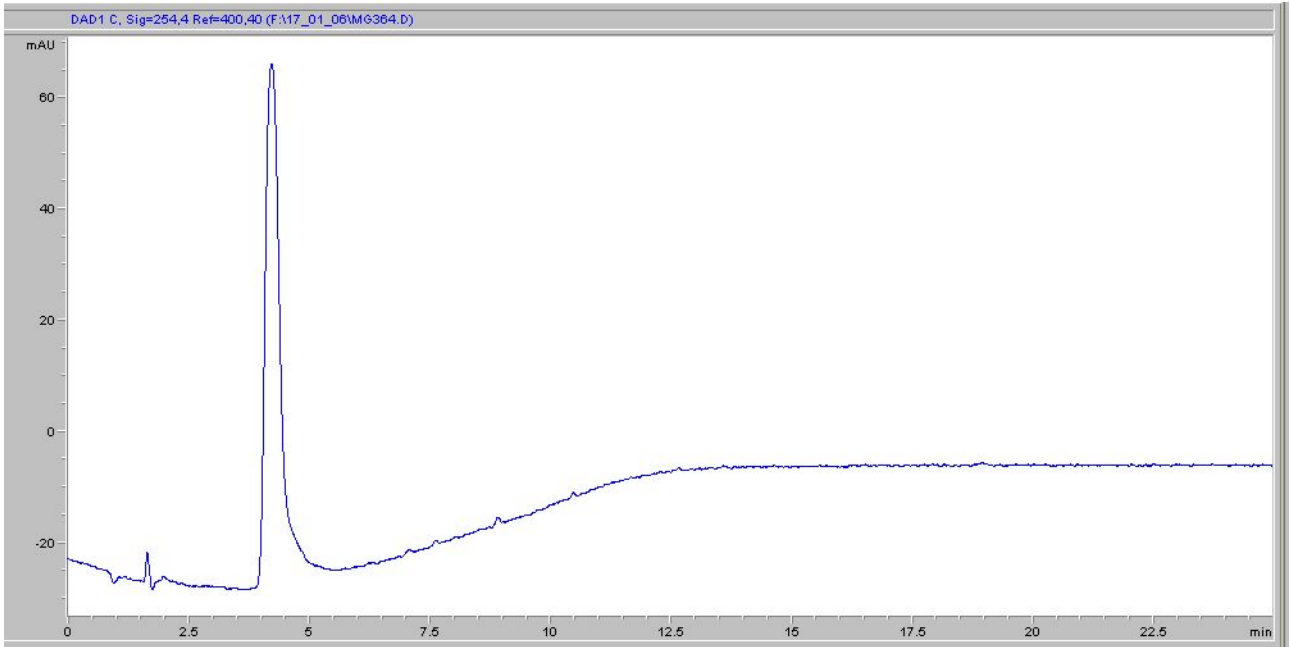
Compound 8



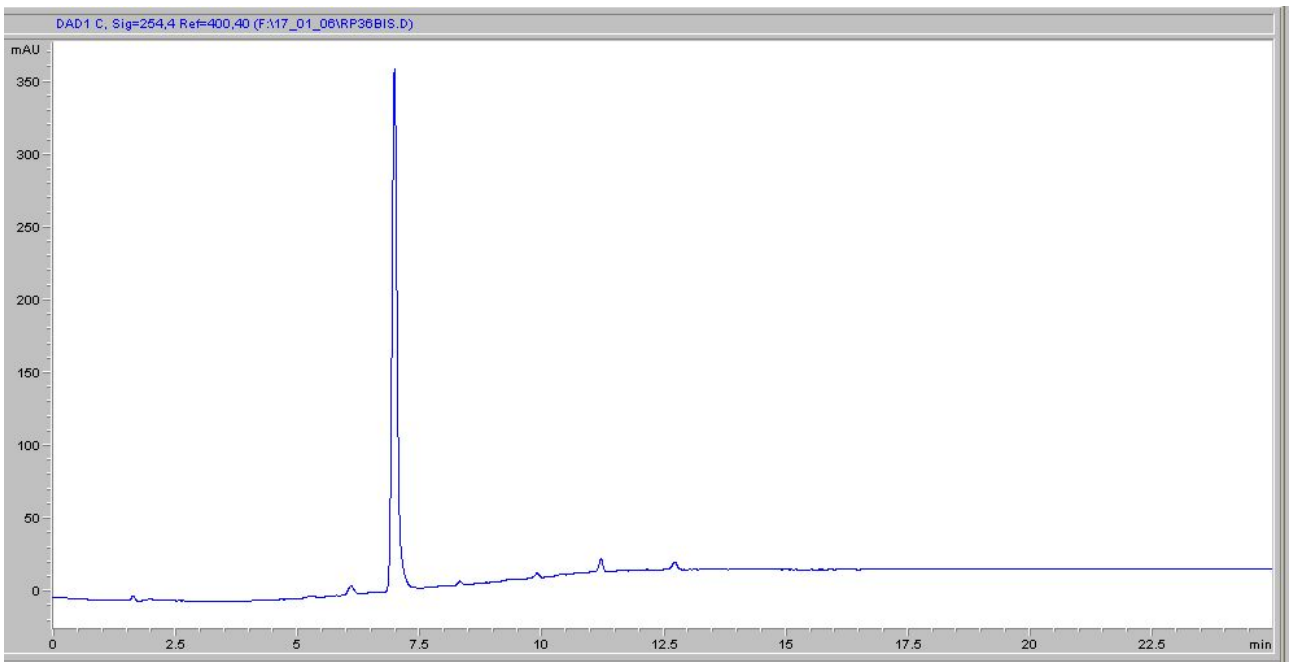
Compound 9



Compound 10



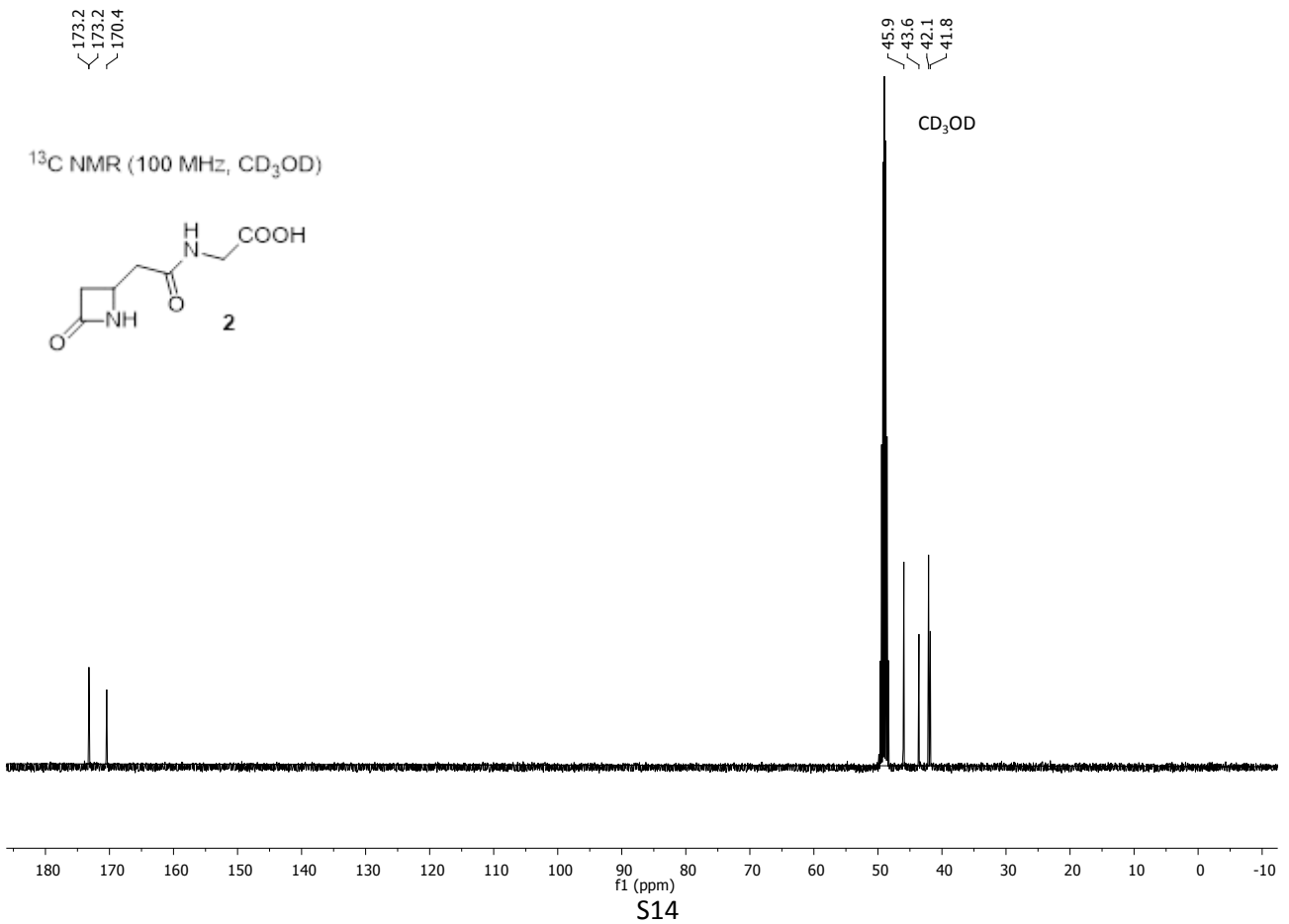
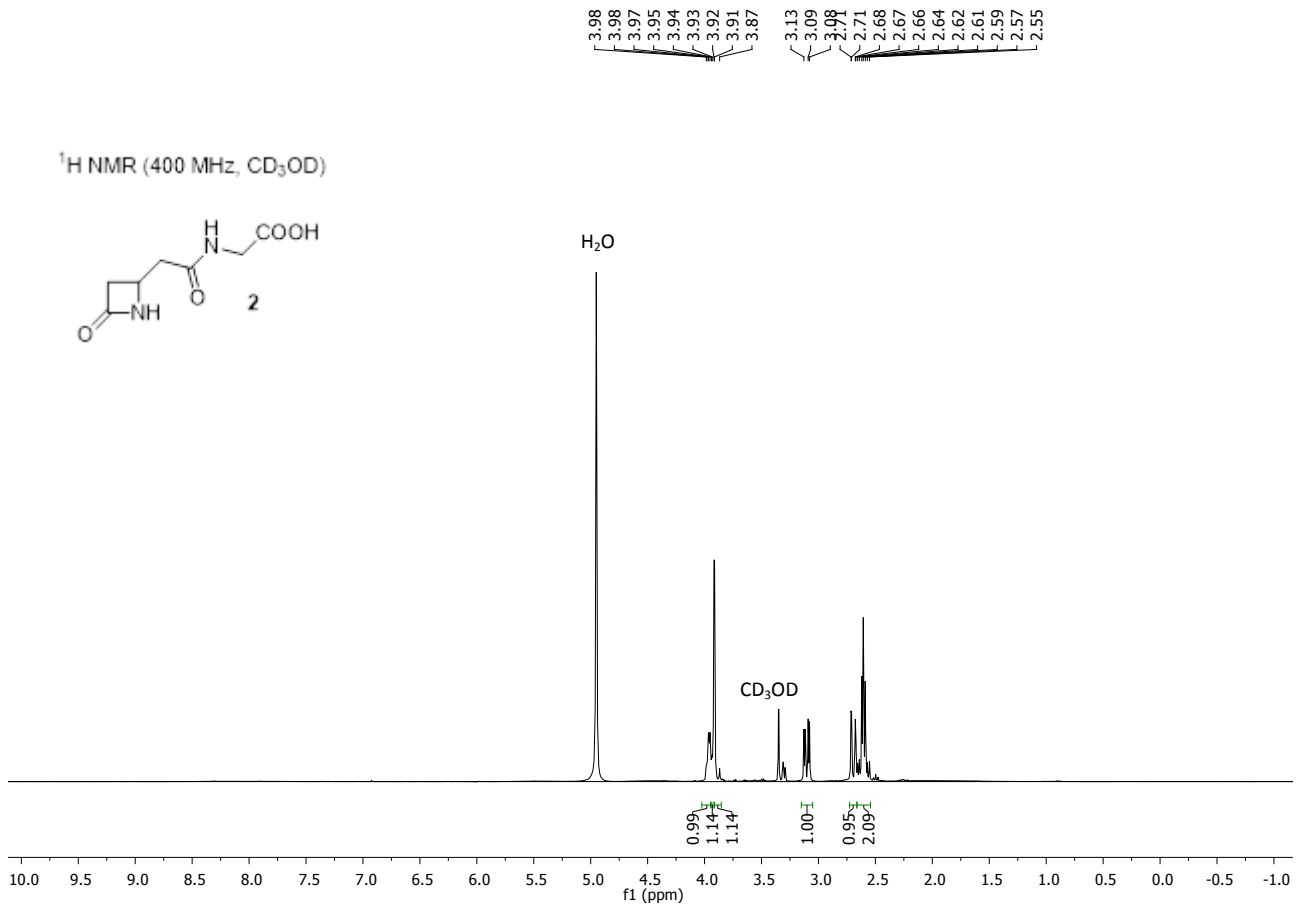
Compound 11



References

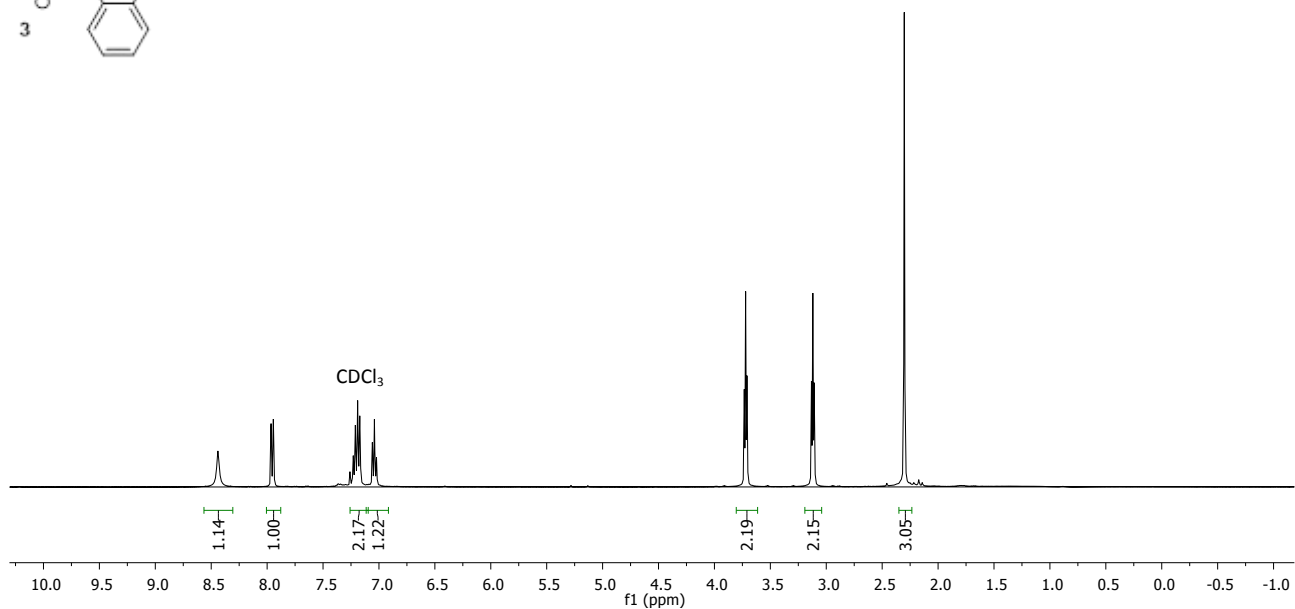
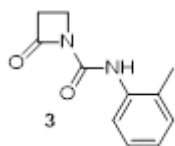
- (1) McKinney, S. A.; Murphy, C. S.; Hazelwood, K. L.; Davidson, M. W.; Looger, L. L. A bright and photostable photoconvertible fluorescent protein. *Nat. Methods* **2009**, *6*, 131–133.
- (2) Baiula, M.; Galletti, P.; Martelli, G.; Soldati, R.; Belvisi, L.; Civera, M.; Dattoli, S. D.; Spampinato S. M.; Giacomini, D. New β -lactam derivatives modulate cell adhesion and signaling mediated by RGD-binding and leukocyte integrins. *J. Med. Chem.* **2016**, *59*, 9721-9742.
- (3) Galletti, P.; Soldati, R.; Pori, M.; Durso, M.; Tolomelli, A.; Gentilucci, L.; Dattoli, S.D.; Baiula, M.; Spampinato, S. M.; Giacomini, D. Targeting integrins $\alpha\beta3$ and $\alpha5\beta1$ with new β -lactam derivatives. *Eur. J. Med. Chem.* **2014**, *83*, 284-293.
- (4) Qasem, A. R.; Bucolo, C.; Baiula, M.; Spartà, A.; Govoni, P.; Bedini, A.; Fasci, D.; Spampinato, S. Contribution of $\alpha4\beta1$ integrin to the antiallergic effect of levocabastine. *Biochem. Pharmacol.* **2008**, *76*, 751–762.
- (5) Dattoli SD, Baiula M, De Marco R, Bedini A, Anselmi M, Gentilucci L, Spampinato S. DS-70, a novel and potent $\alpha(4)$ integrin antagonist, is an effective treatment for experimental allergic conjunctivitis in guinea pigs. *Br J Pharmacol.* **2018** Oct;175(20):3891-3910.
- (6) Bedini A, Baiula M, Spampinato S. Transcriptional activation of human mu-opioid receptor gene by insulin-like growth factor-I in neuronal cells is modulated by the transcription factor REST. *J Neurochem.* **2008** Jun 1;105(6):2166-78.
- (7). Word, J. M.; Lovell, S. C.; Richardson, J. S.; David C. Richardson, D. C. Asparagine and glutamine: using hydrogen atom contacts in the choice of side-chain amide orientation. *J. Mol. Biol.* **1999**, *285*, 1735-1747.
- (8). Olsson, M. H. M.; Søndergaard, C. R.; Rostkowski, M.; Jensen, J. H. PROPKA3: Consistent Treatment of Internal and Surface Residues in Empirical pKa Predictions. *J. Chem. Theory Comput.* **2011**, *7*, 525-537.
- (9). Huey, R.; Morris, G. M.; Olson, A. J.; Goodsell, D. S. A semiempirical free energy force field with charge-based desolvation. *J. Comput. Chem.* **2007**, *28*, 1145-1152.
- (10). Solis, F. J.; Wets, R. J.-B. Minimization by Random Search Techniques. *Math. Oper. Res.* **1981**, *6*, 19-30.
- (11). Sanner, M. F. Py–thon: a programming language for software integration and development. *J. Mol. Graph. Model.* **1999**, *17*, 57-61.
- (12). Gasteiger, J.; Marsili, M. Iterative partial equalization of orbital electronegativity—a rapid access to atomic charges. *Tetrahedron* **1980**, *36*, 3219-3228.

(13). Xiong JP, Stehle T, Zhang R, Joachimiak A, Frech M, Goodman SL et al. Crystal structure of the extracellular segment of integrin α V β 3 in complex with an Arg-Gly-Asp ligand. *Science* 2002, 296, 151–155.



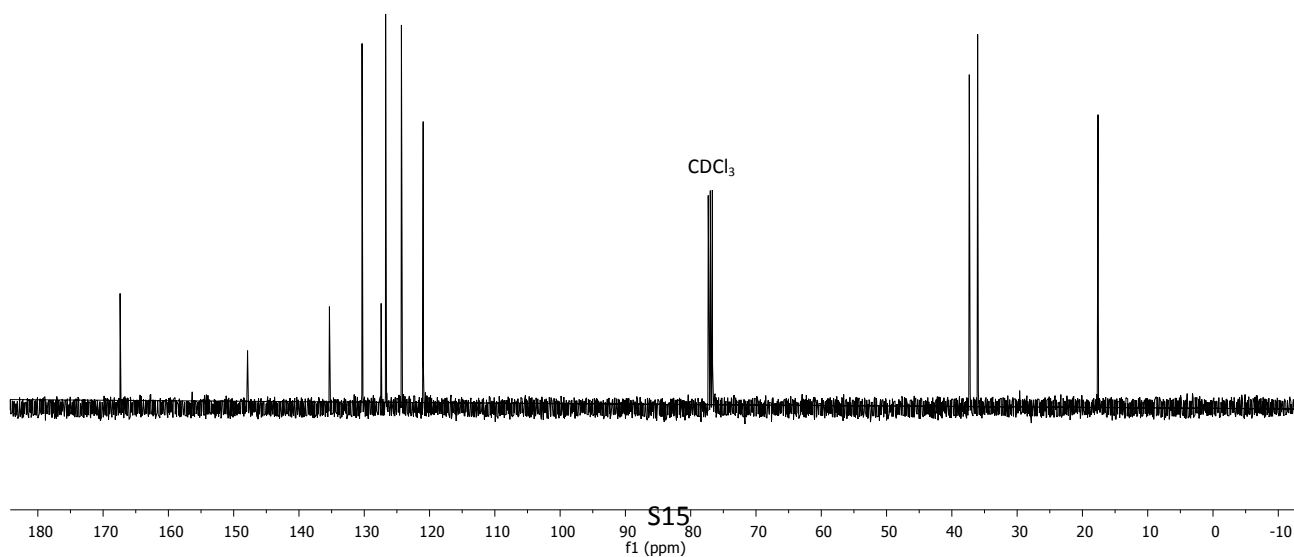
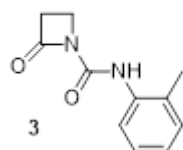
8.44
7.96
7.94
7.23
7.21
7.19
7.17
7.06
7.04
7.02
3.73
3.72
3.71
3.13
3.12
3.11
2.30

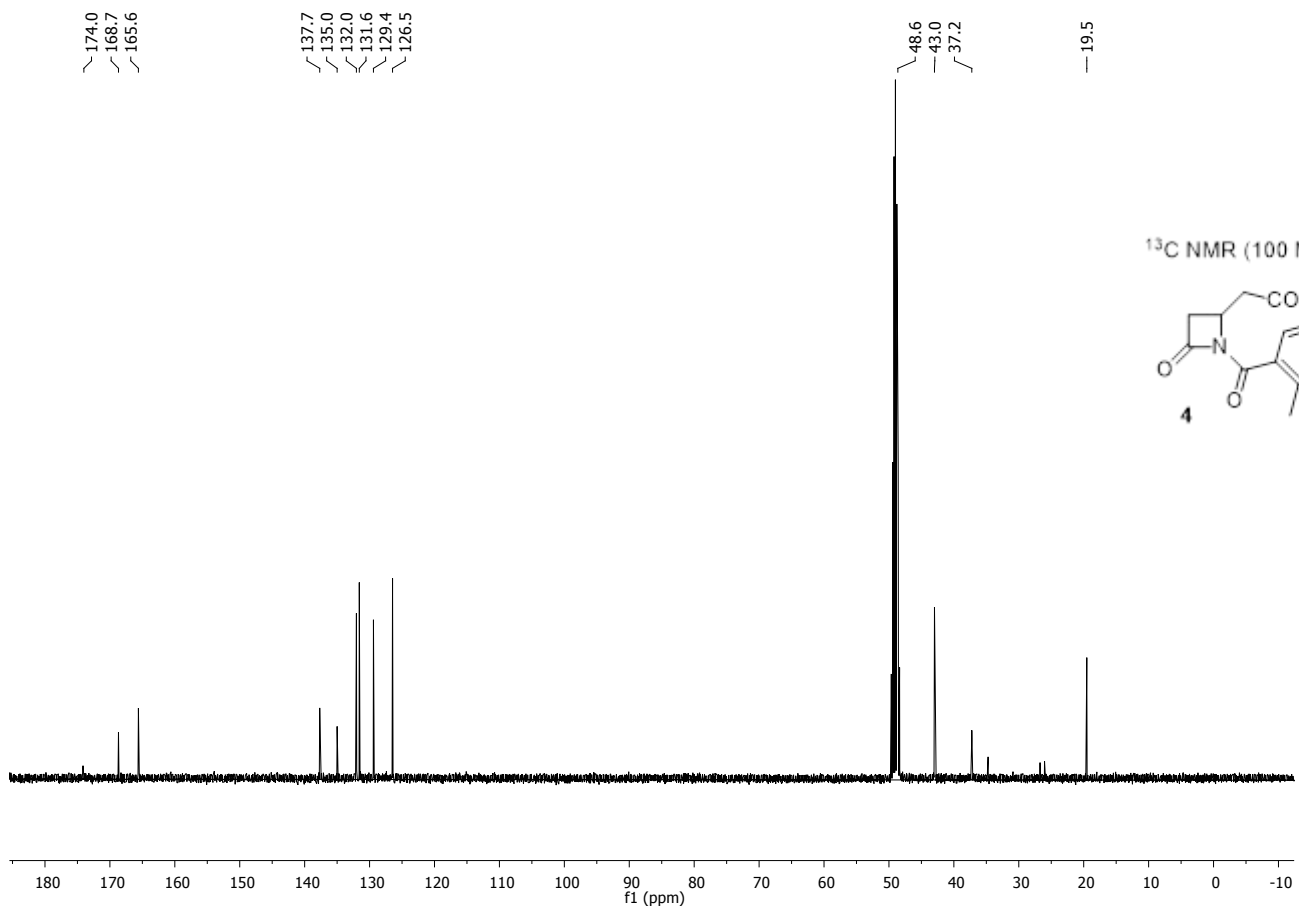
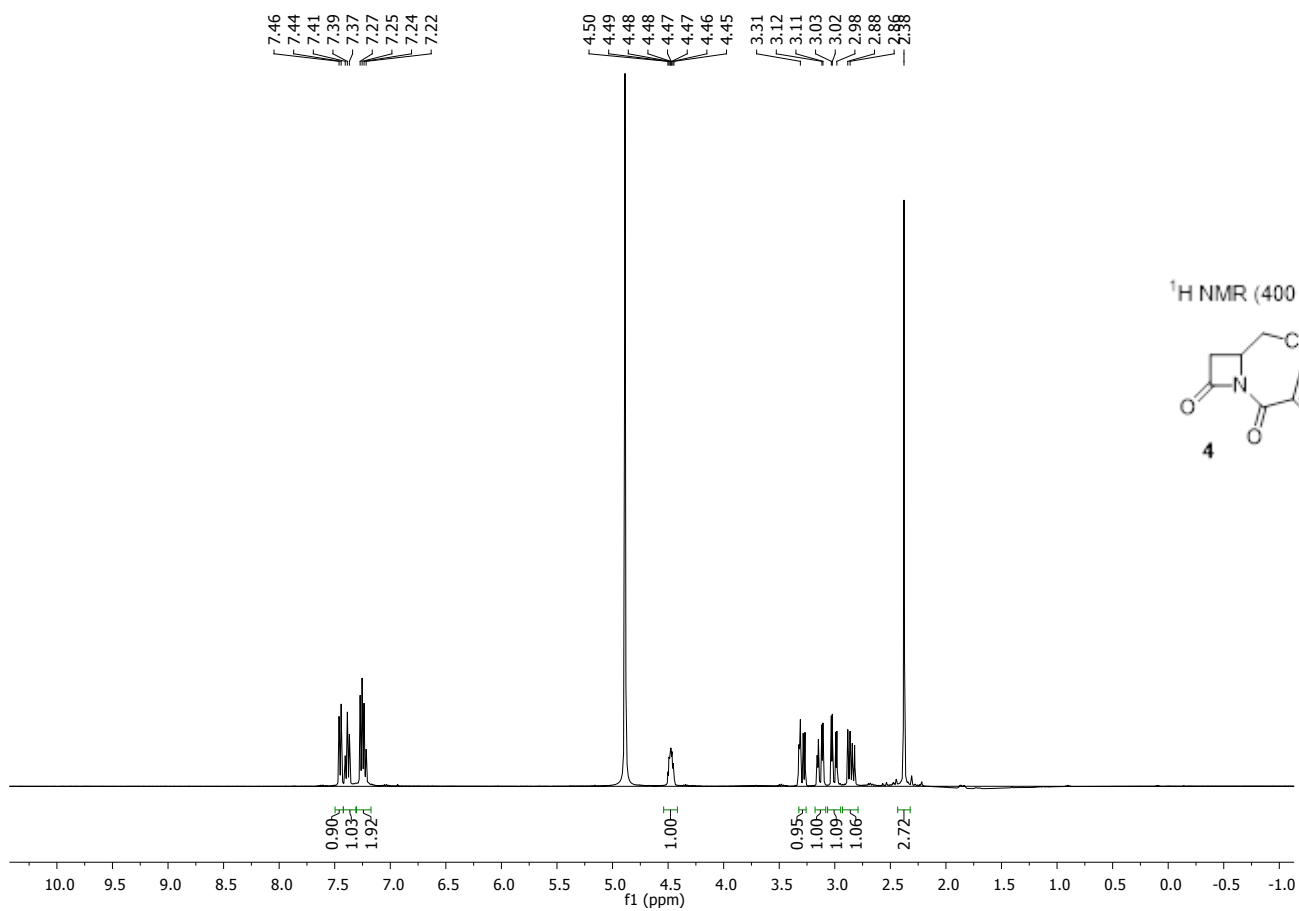
¹H NMR (400 MHz, CDCl₃)

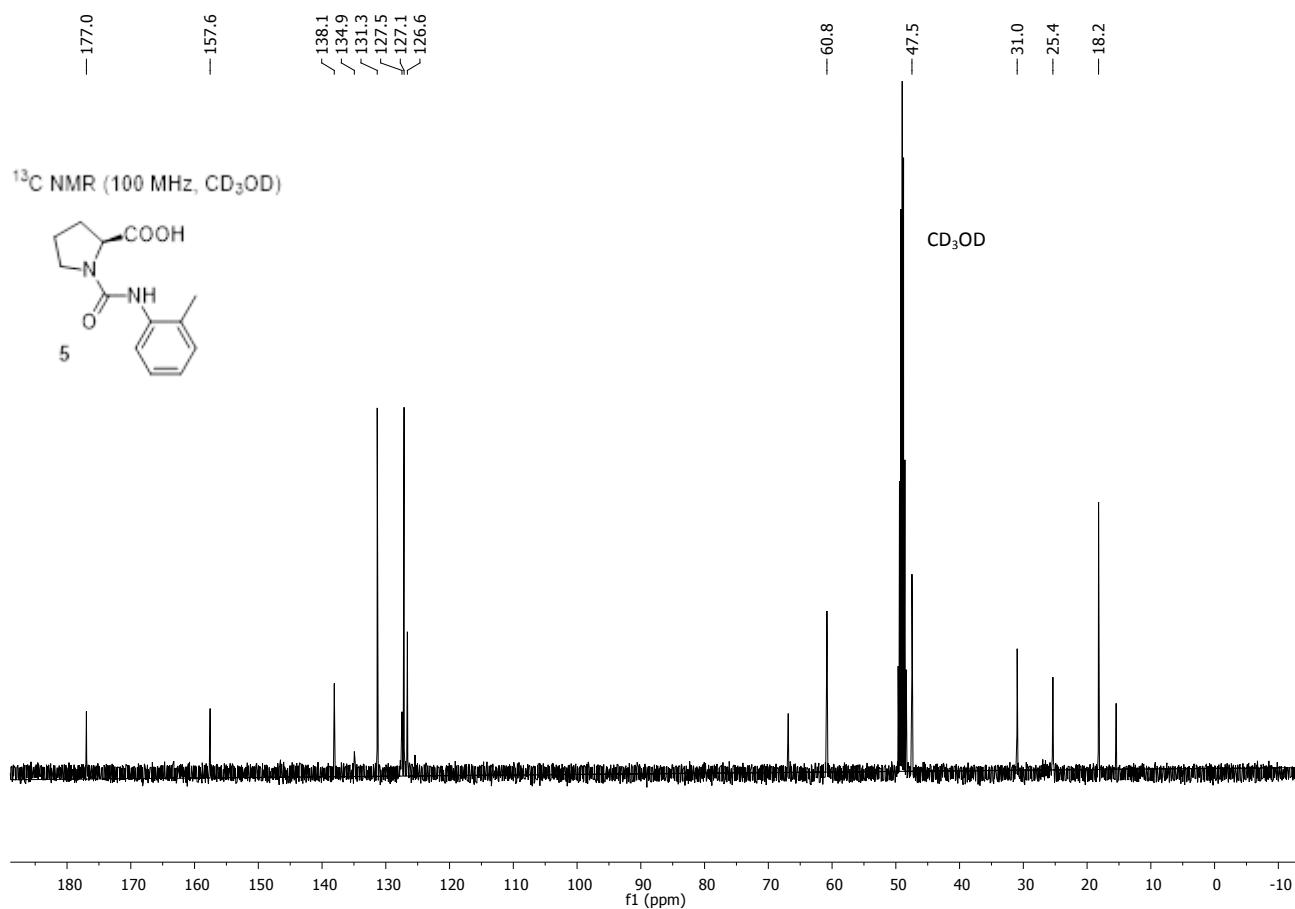
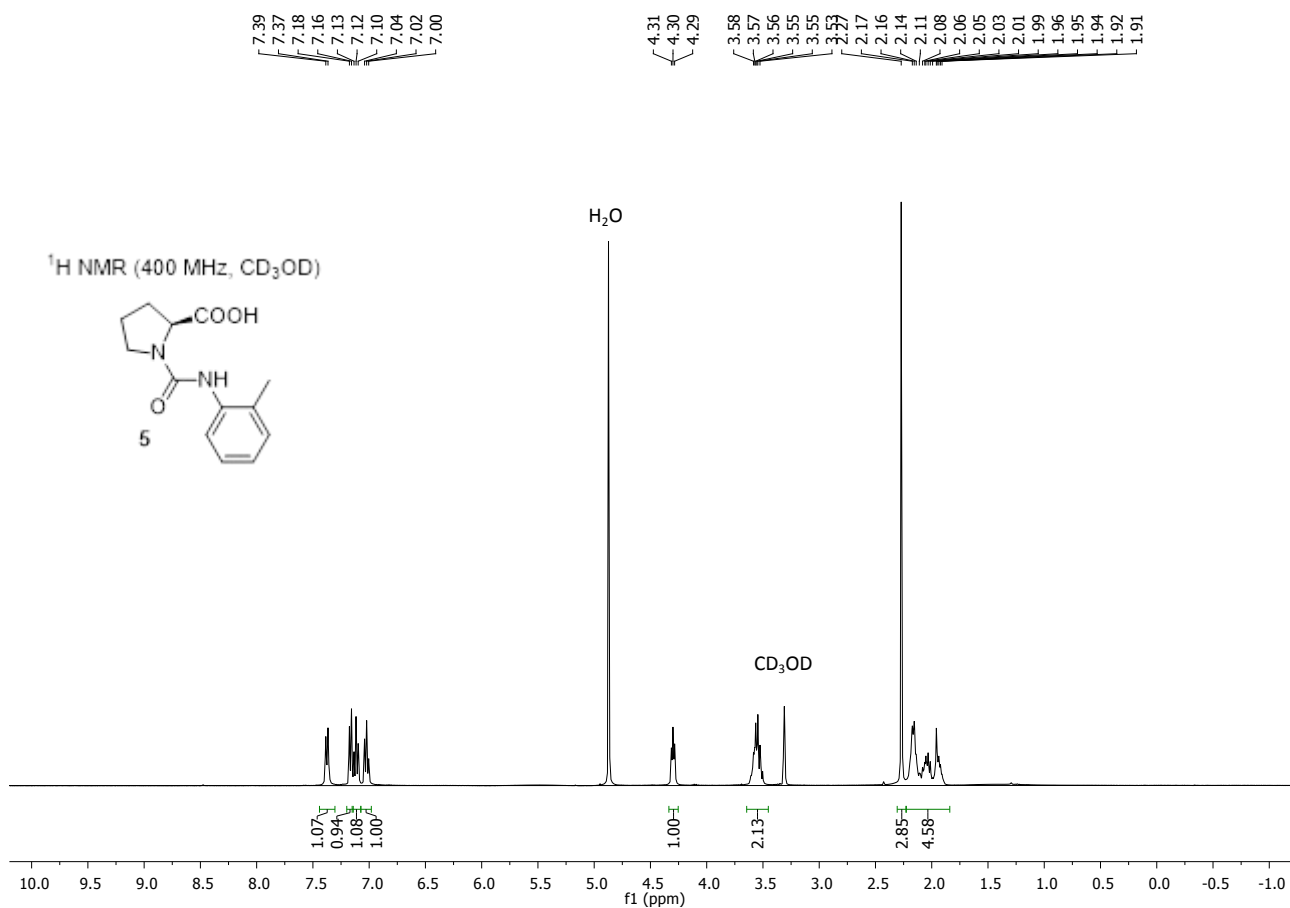


167.4
147.9
135.3
130.3
127.4
126.7
124.3
121.0
37.3
36.0
17.6

¹³C NMR (100 MHz, CDCl₃)





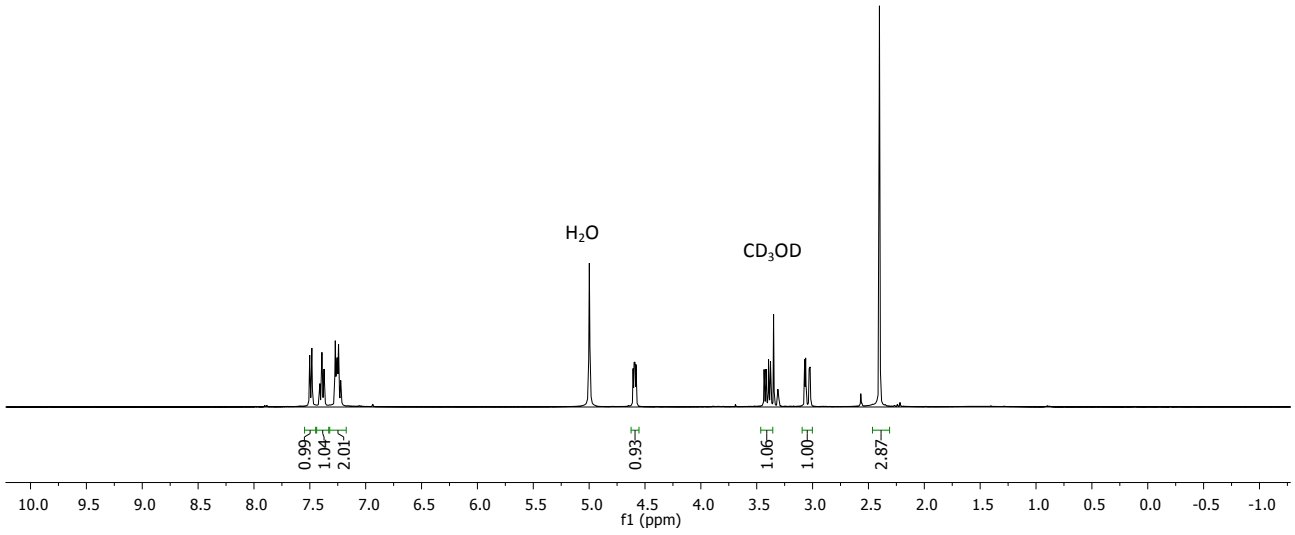
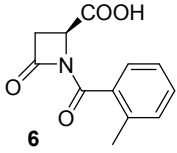


7.50
7.48
7.41
7.39
7.37
7.27
7.26
7.25
7.24
7.22

4.61
4.60
4.59
4.58

3.43
3.42
3.39
3.38
3.07
3.06
3.02
2.40

¹H NMR (400 MHz, CD₃OD)



172.9
167.7
164.0

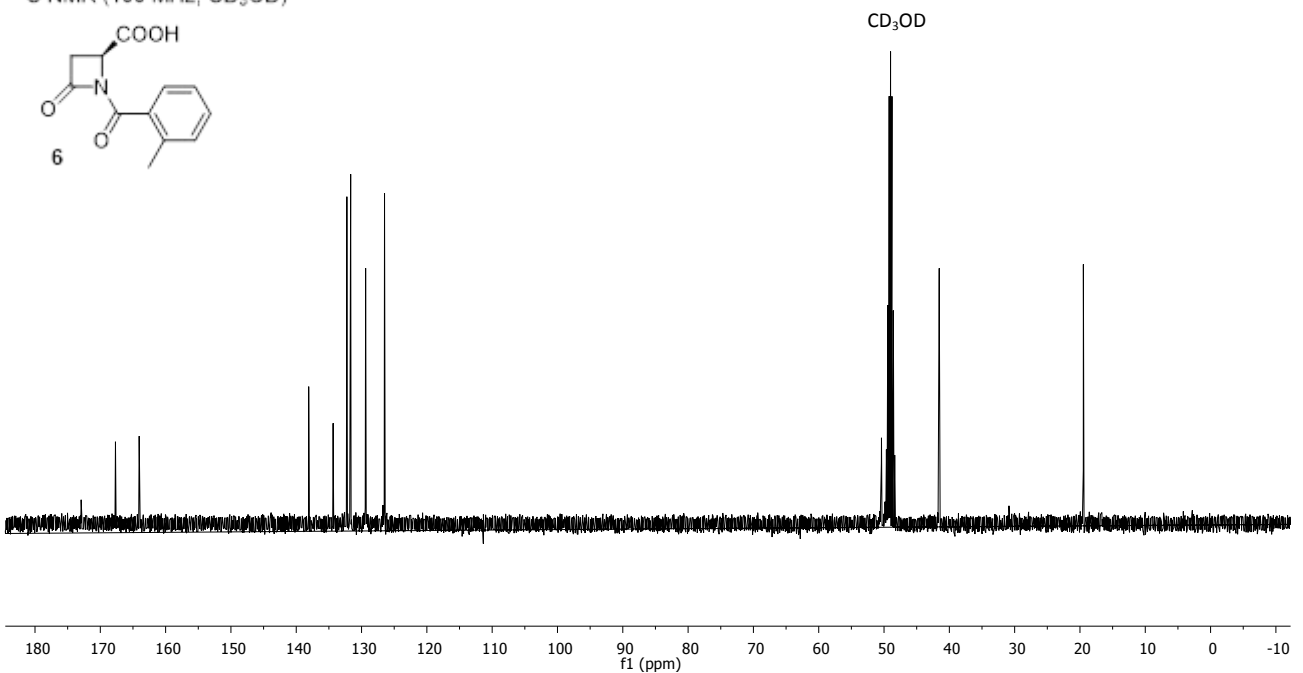
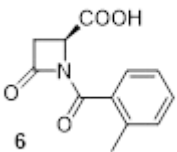
138.1
134.4
132.2
131.7
129.4
126.5

50.4

41.5

19.5

¹³C NMR (100 MHz, CD₃OD)

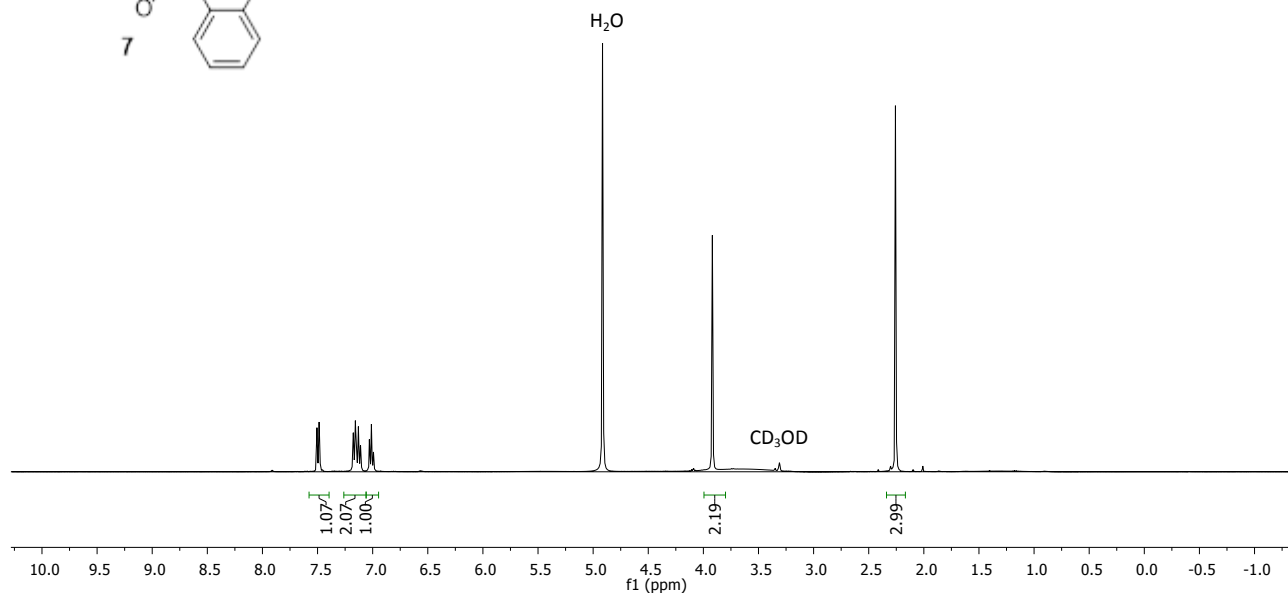
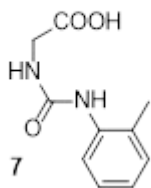


7.51
7.49
7.18
7.16
7.13
7.11
7.03
7.01
6.99

3.92

2.26

¹H NMR (400 MHz, CD₃OD)



172.8

157.2

136.6

130.4

130.0

126.0

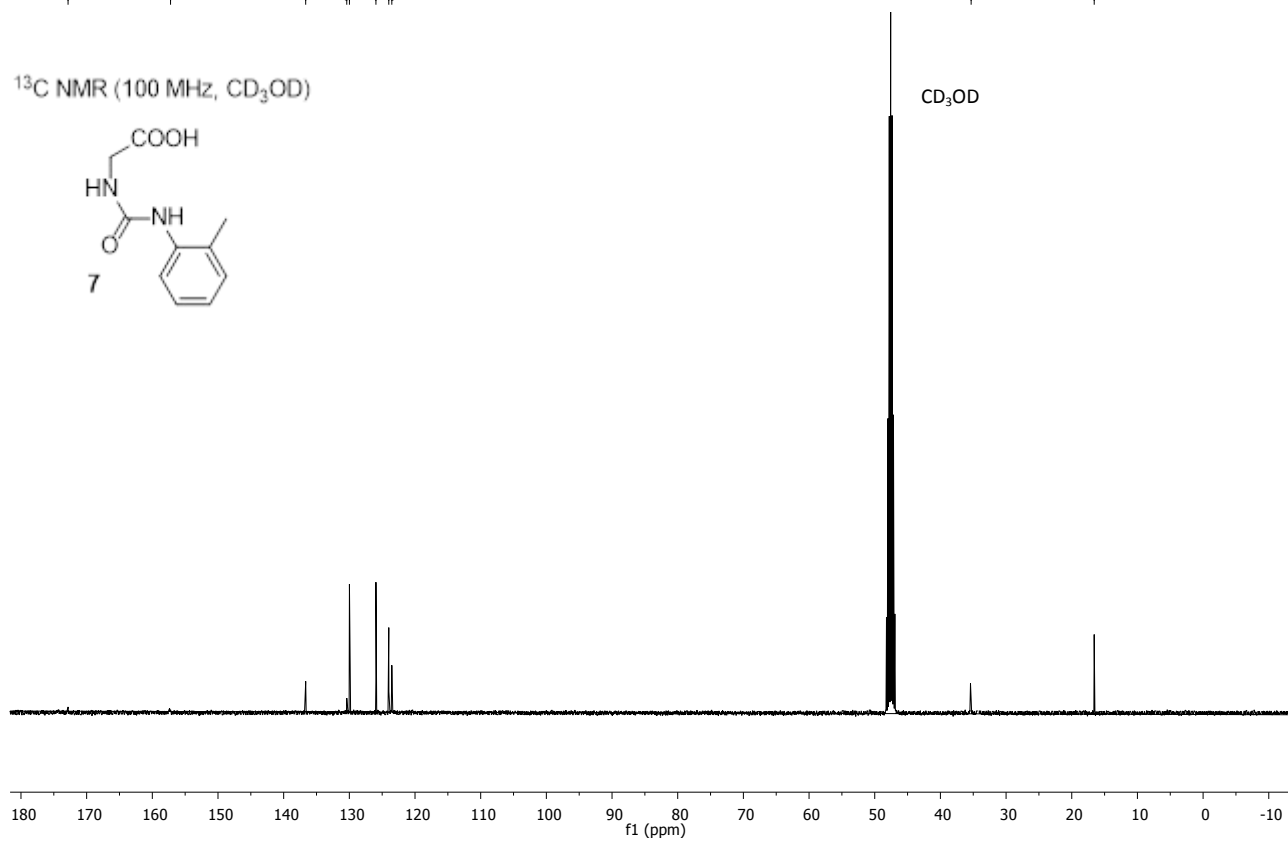
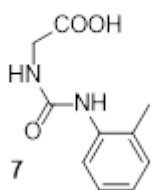
124.0

123.5

35.3

16.6

¹³C NMR (100 MHz, CD₃OD)

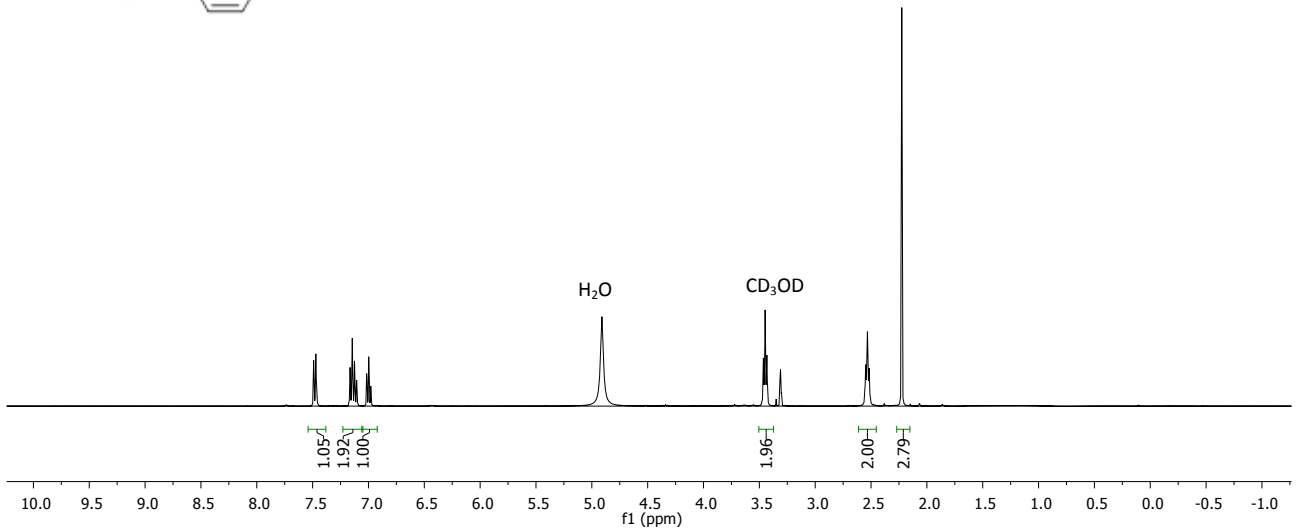
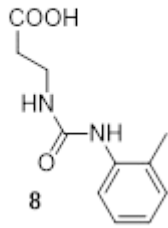


7.49
7.47
7.16
7.14
7.13
7.11
7.02
7.00
6.98

3.46
3.45
3.43

2.55
2.53
2.52
2.23

¹H NMR (400 MHz, CD₃OD)



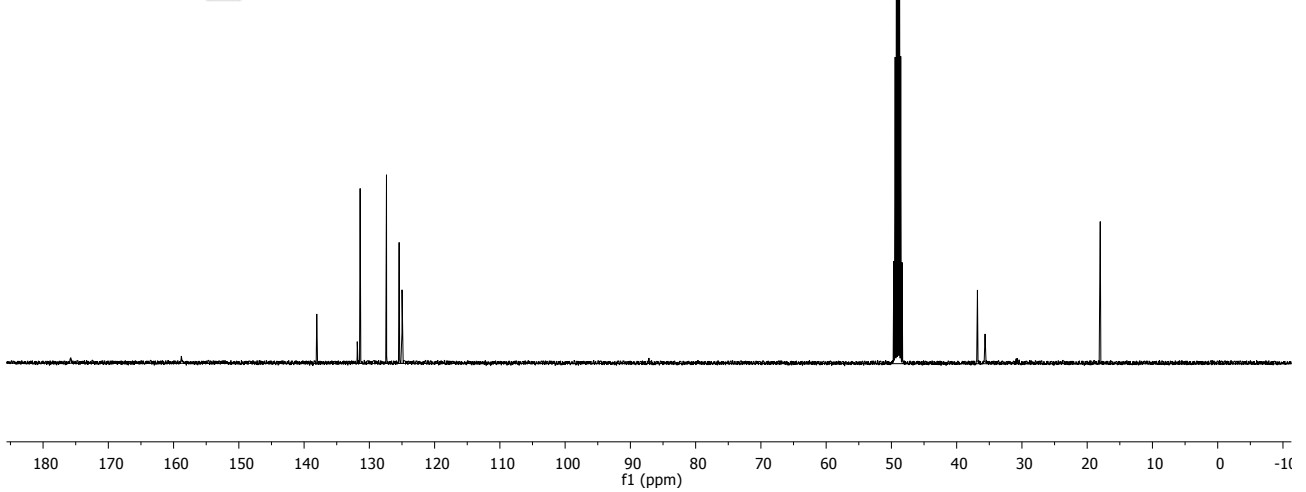
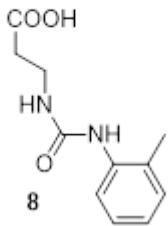
175.8
158.8
138.1
131.9
131.4
127.4
125.4
125.0

CD₃OD

36.8
35.6

18.0

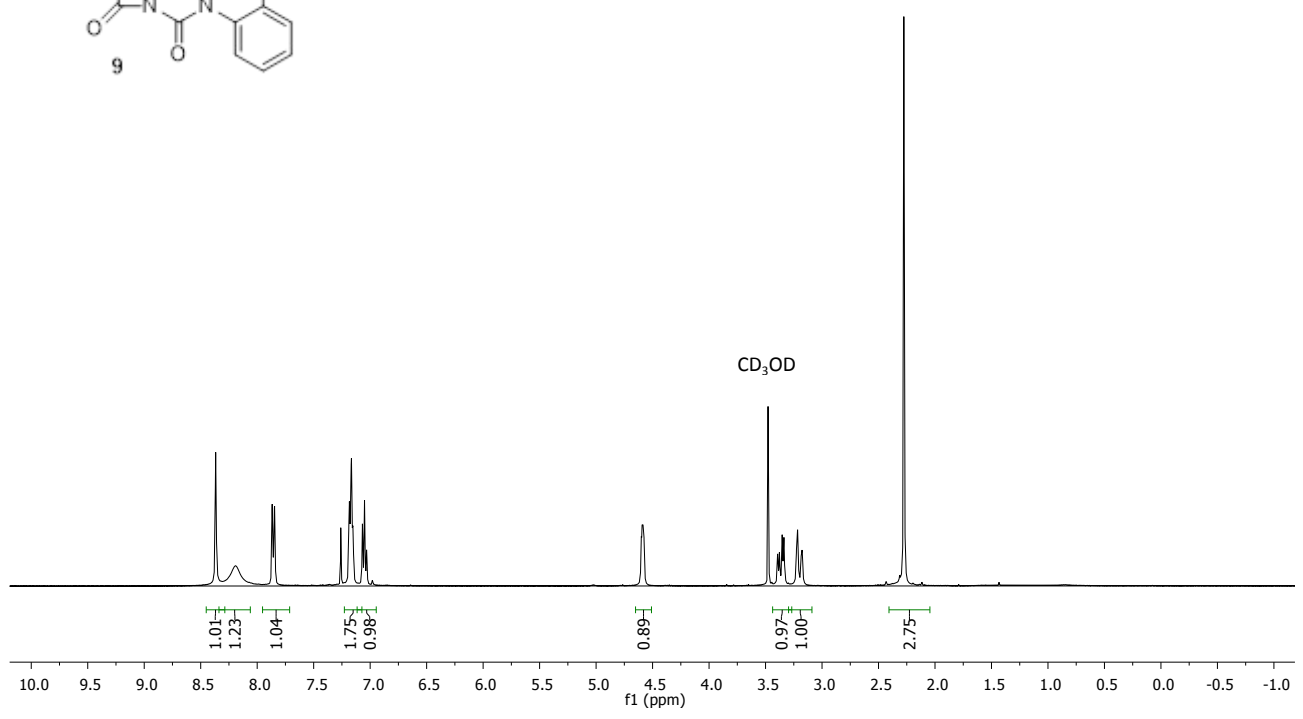
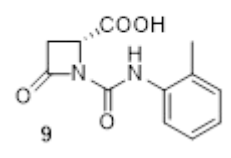
¹³C NMR (100 MHz, CD₃OD)



8.37
8.19
7.87
7.85
7.18
7.17
7.15
7.07
7.05
7.03

4.60
4.59
4.58
4.58
3.48
3.39
3.38
3.35
3.34
3.22
3.22
3.18
3.18
2.28

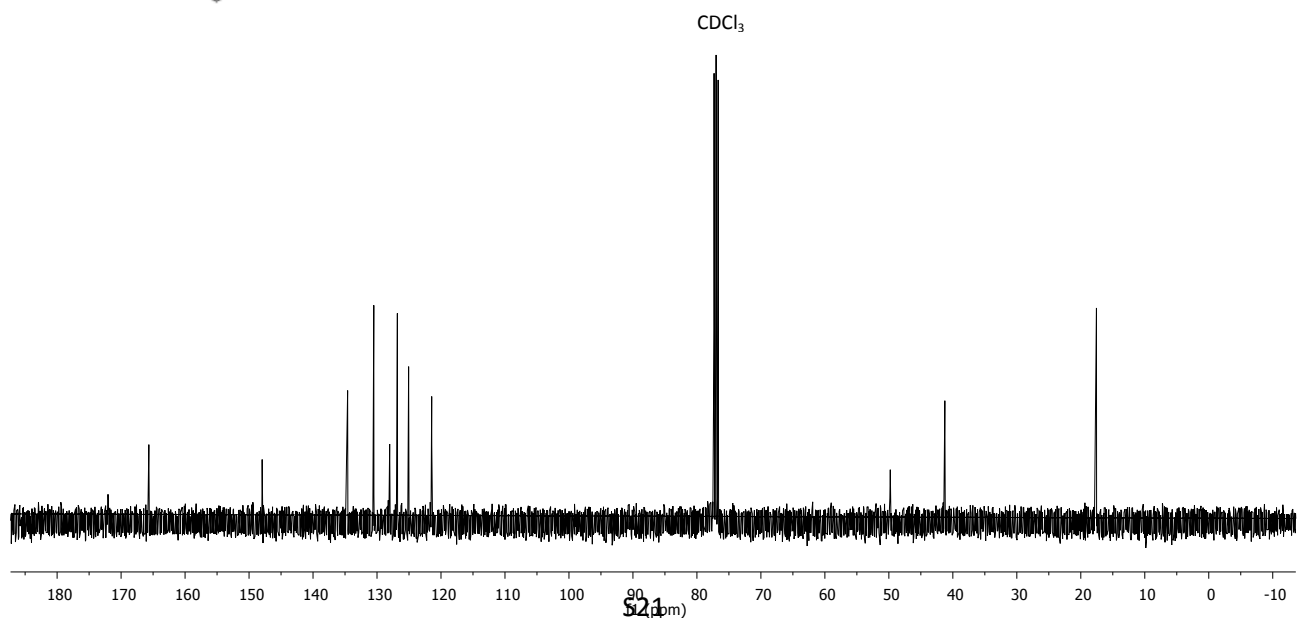
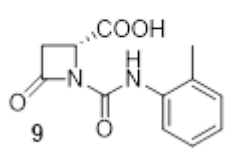
¹H NMR (400 MHz, CD₃OD)



172.0
165.7
147.9
134.6
130.5
128.0
126.8
125.1
121.5

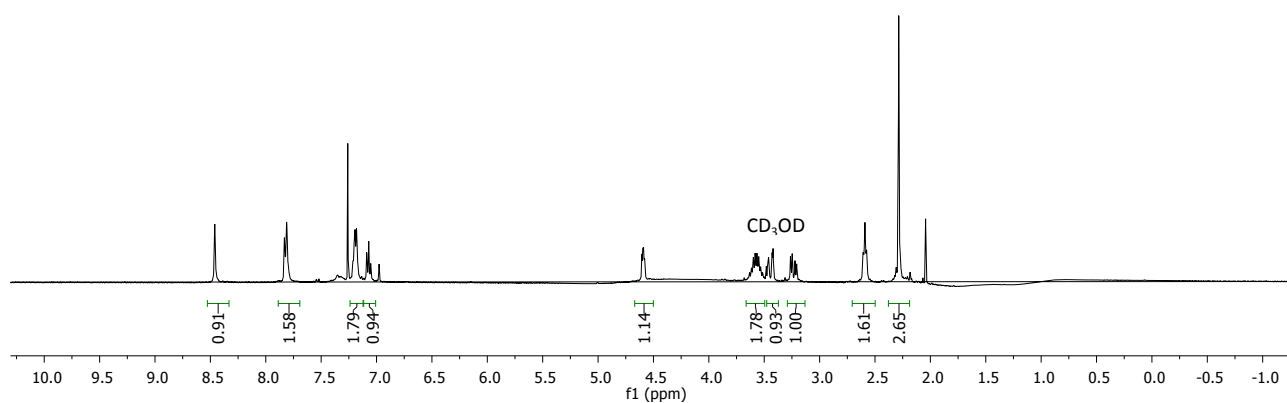
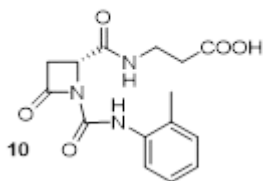
49.7
41.3
17.6

¹³C NMR (100 MHz, CDCl₃)



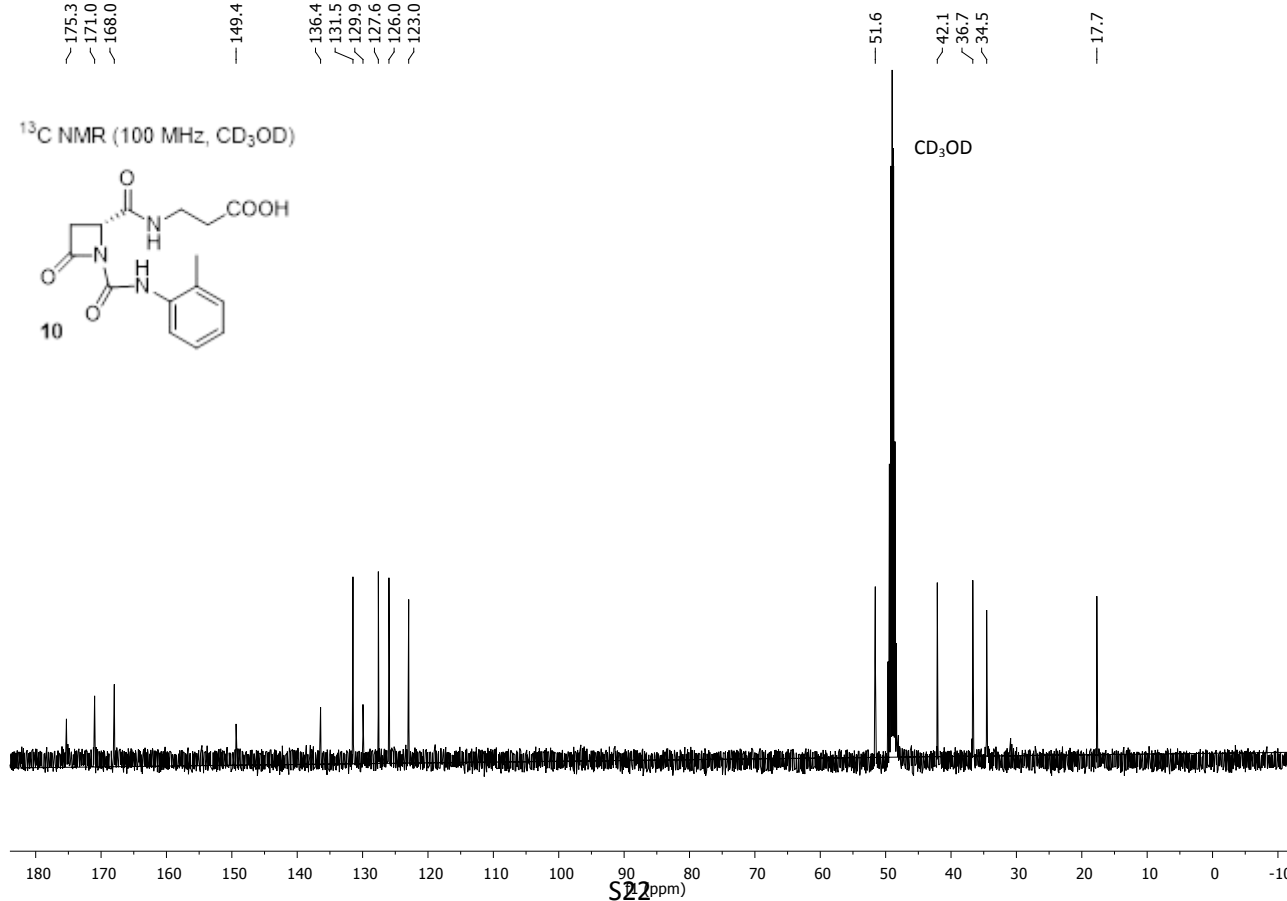
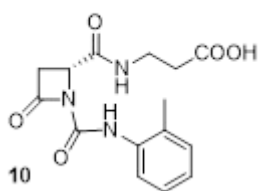
8.46
 7.83
 7.81
 7.21
 7.19
 7.18
 7.09
 7.07
 7.05
 4.60
 4.60
 4.59
 4.58
 3.60
 3.58
 3.57
 3.55
 3.43
 3.42
 3.26
 3.25
 2.60
 2.59
 2.58
 2.29

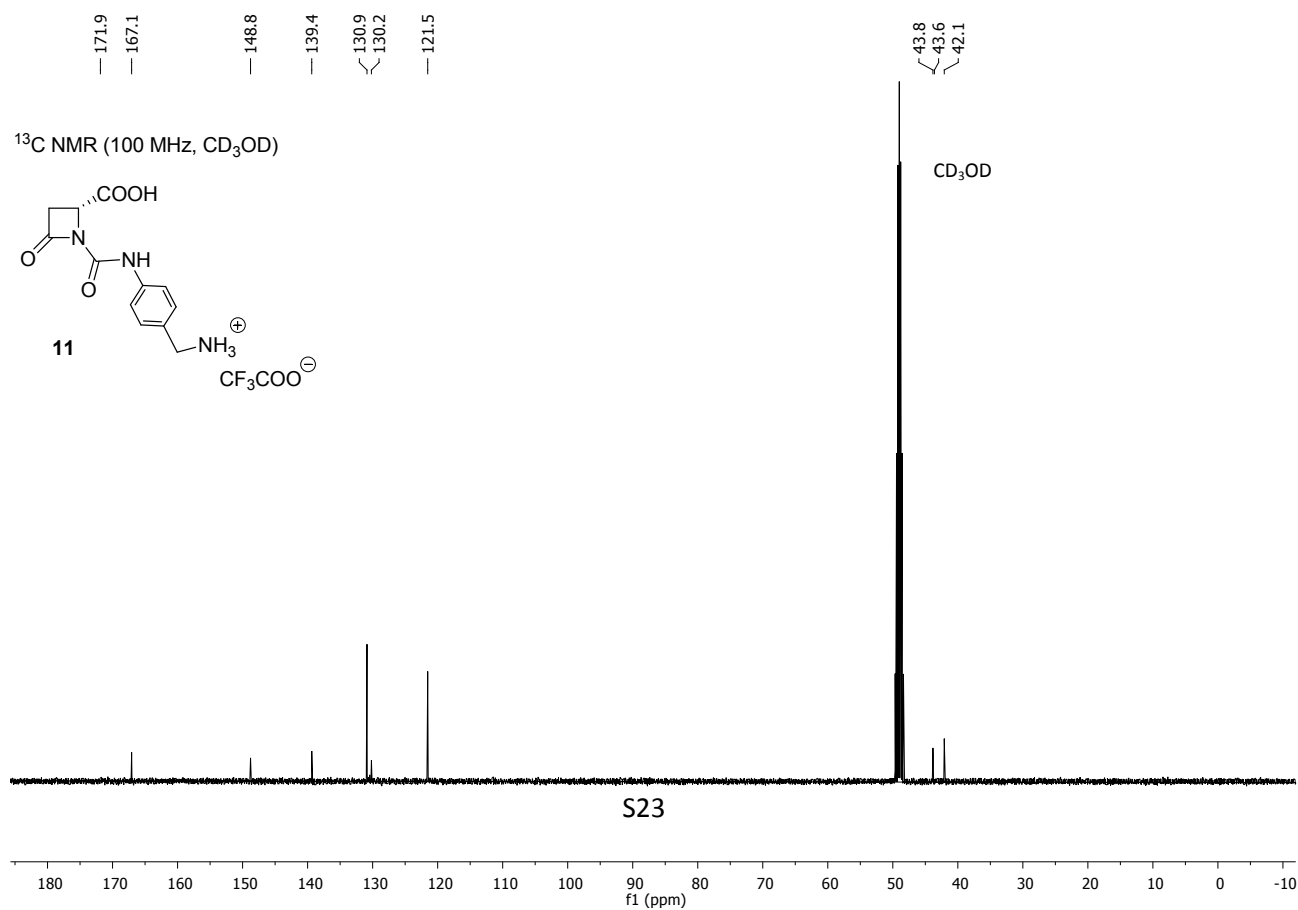
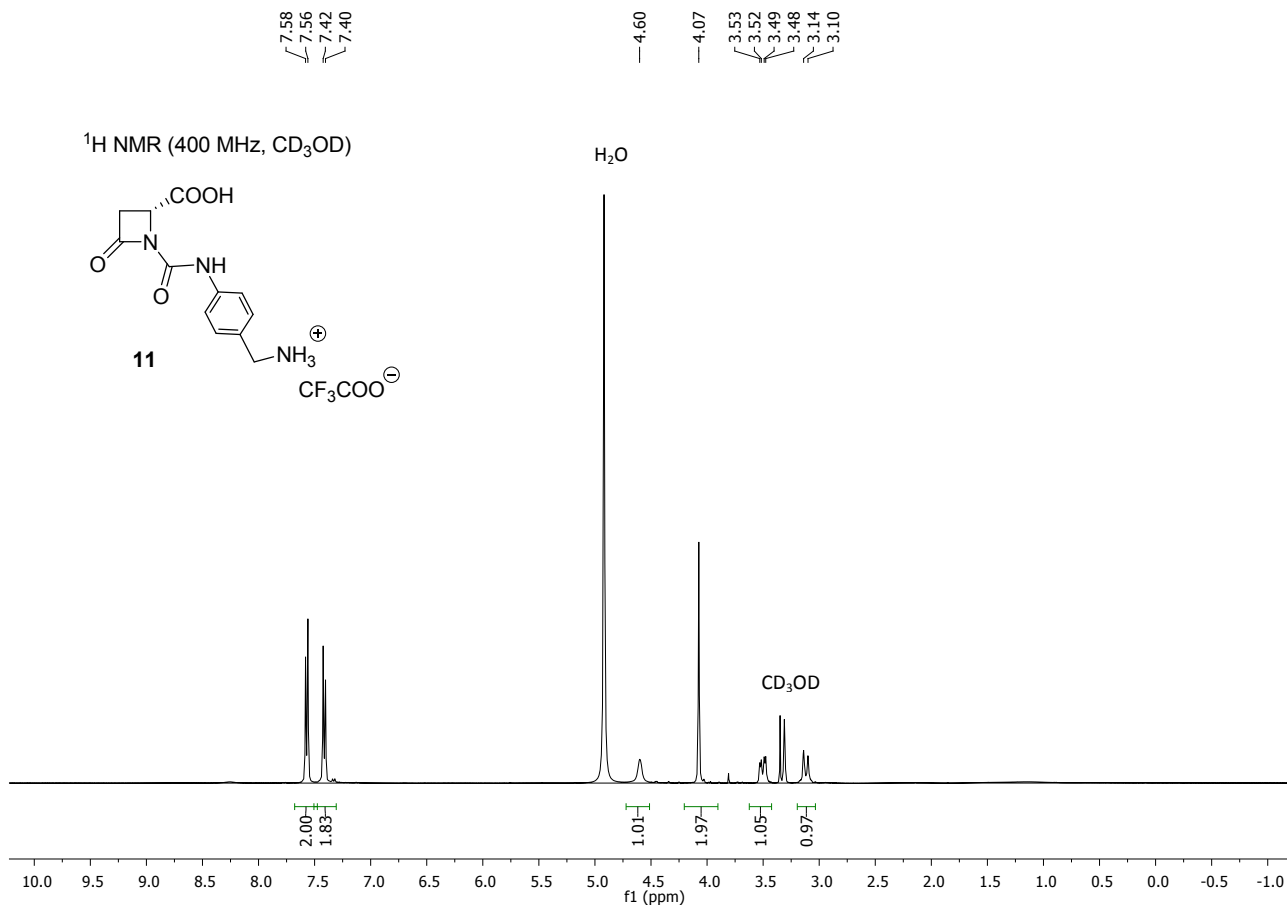
¹H NMR (400 MHz, CD₃OD)

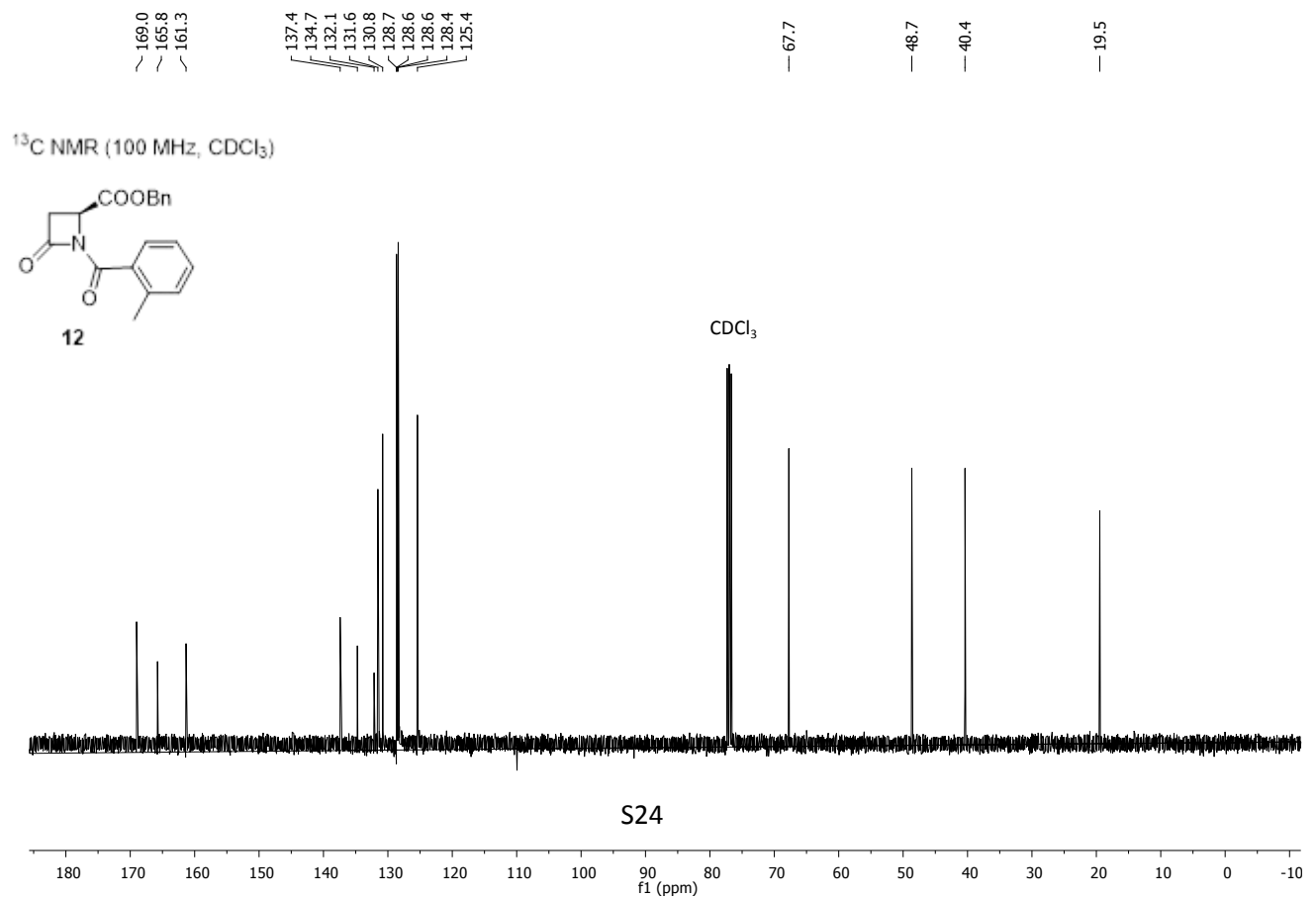
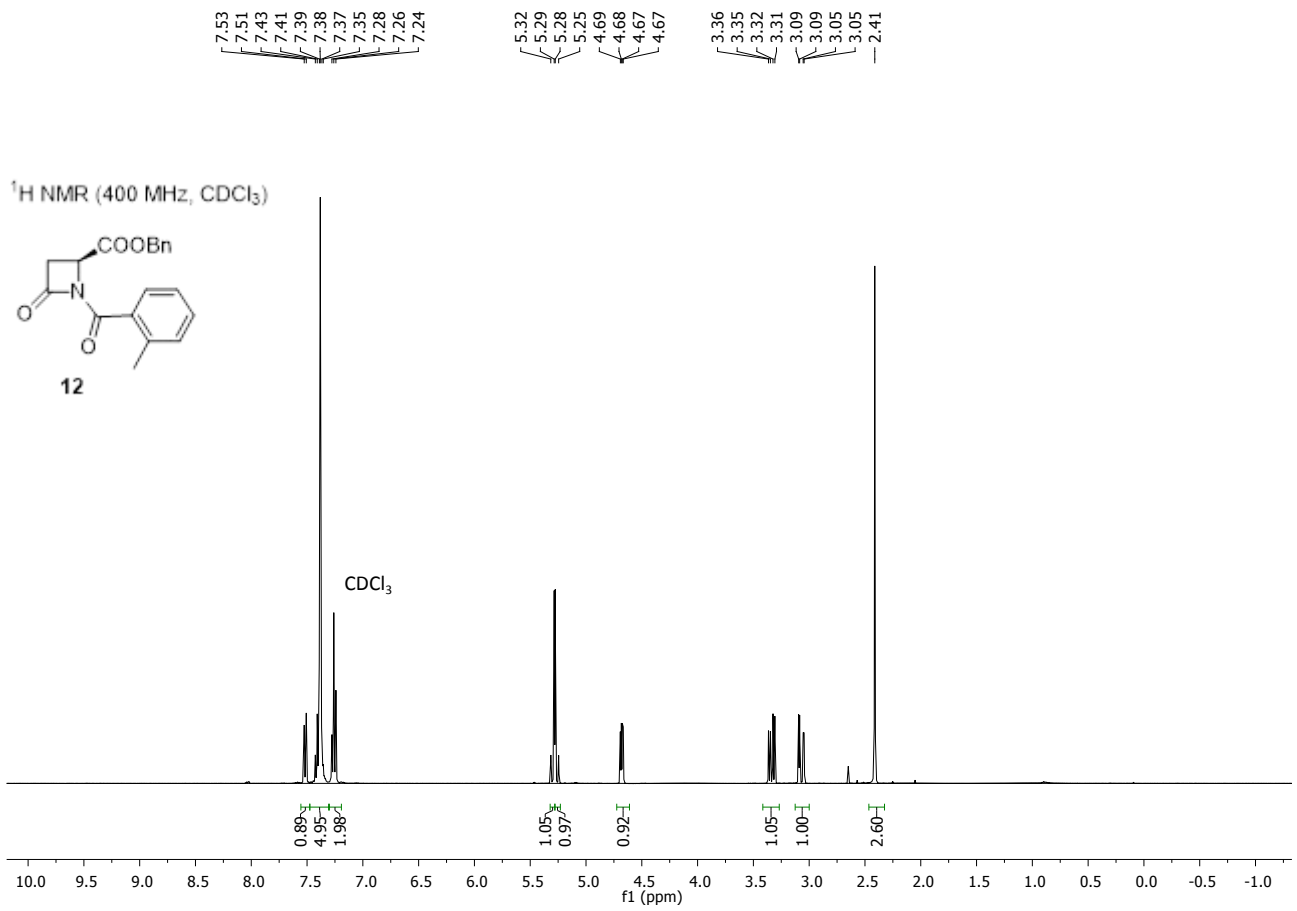


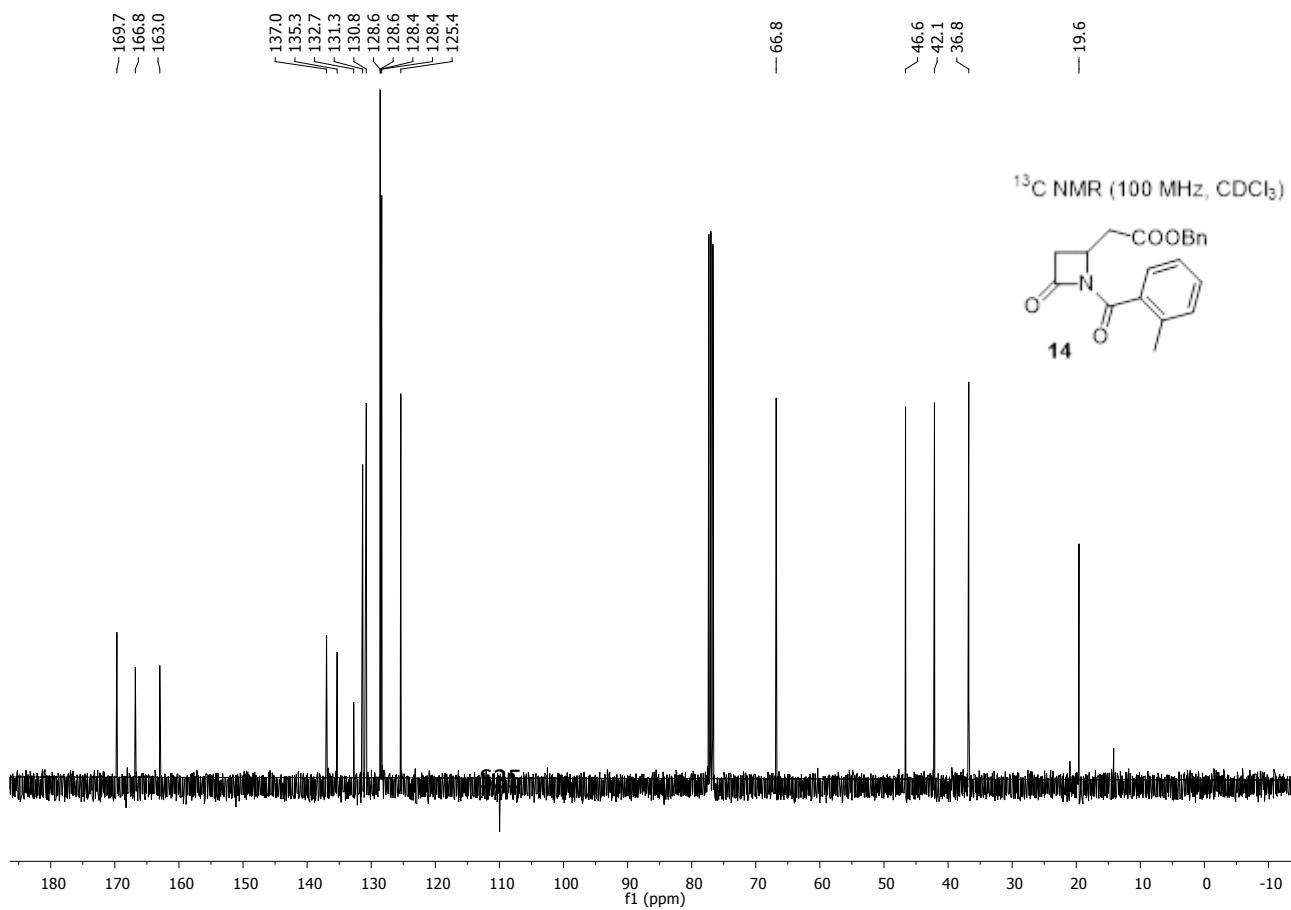
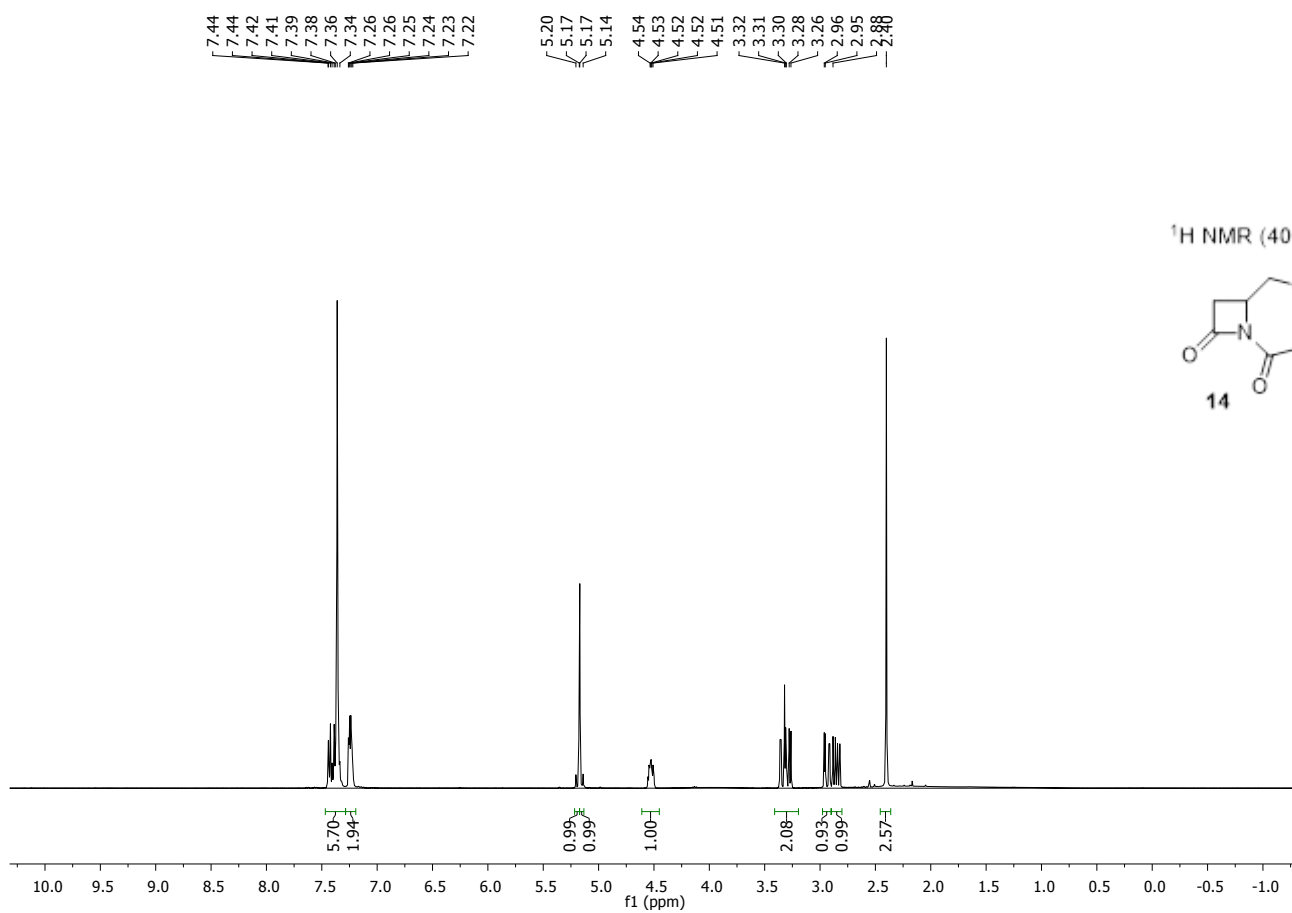
175.3
 171.0
 168.0
 149.4
 136.4
 131.5
 129.9
 127.6
 126.0
 123.0

¹³C NMR (100 MHz, CD₃OD)



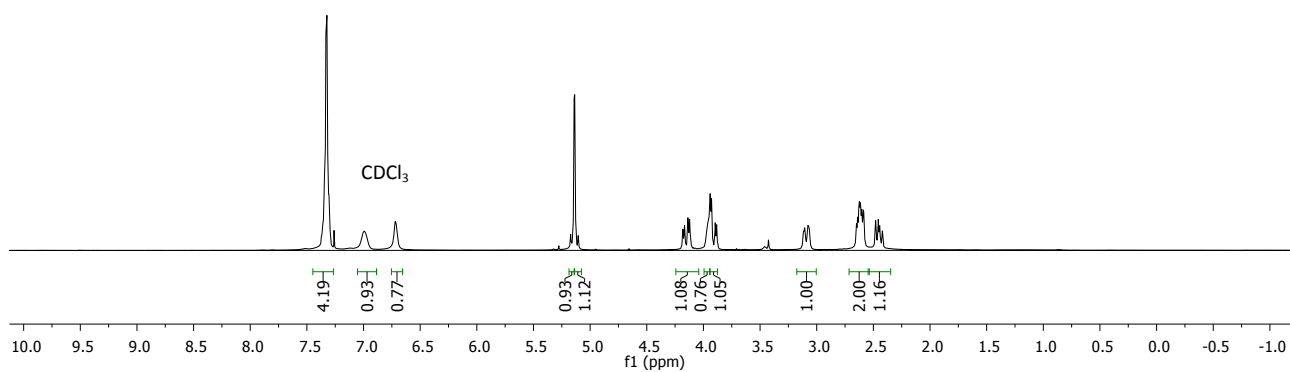
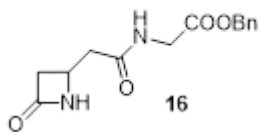






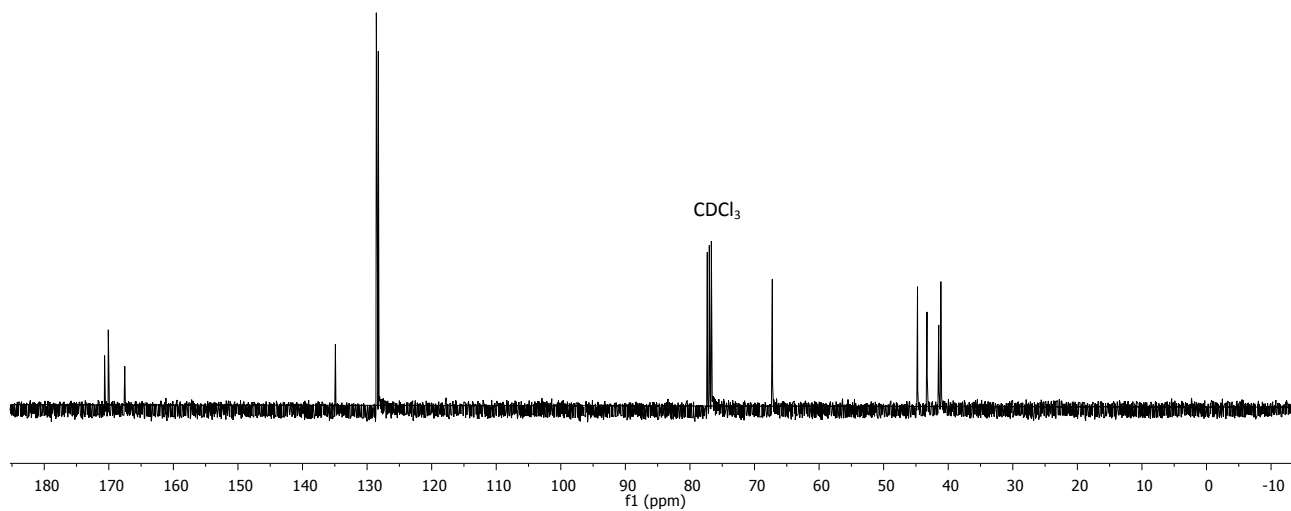
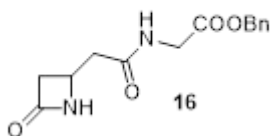
7.37, 7.36, 7.34, 7.34, 7.33, 7.32, 7.31, 6.99, 6.72, 5.17, 5.14, 5.14, 5.11, 4.17, 4.14, 4.12, 3.94, 3.93, 3.90, 3.88, 3.11, 3.08, 2.65, 2.64, 2.62, 2.61, 2.60, 2.59, 2.48, 2.46, 2.44, 2.42

¹H NMR (400 MHz, CDCl₃)

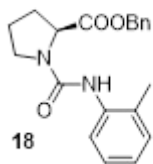


170.7, 170.1, 167.5, 134.9, 128.6, 128.5, 128.3, 67.2, 44.8, 43.3, 41.5, 41.1

¹³C NMR (100 MHz, CDCl₃)



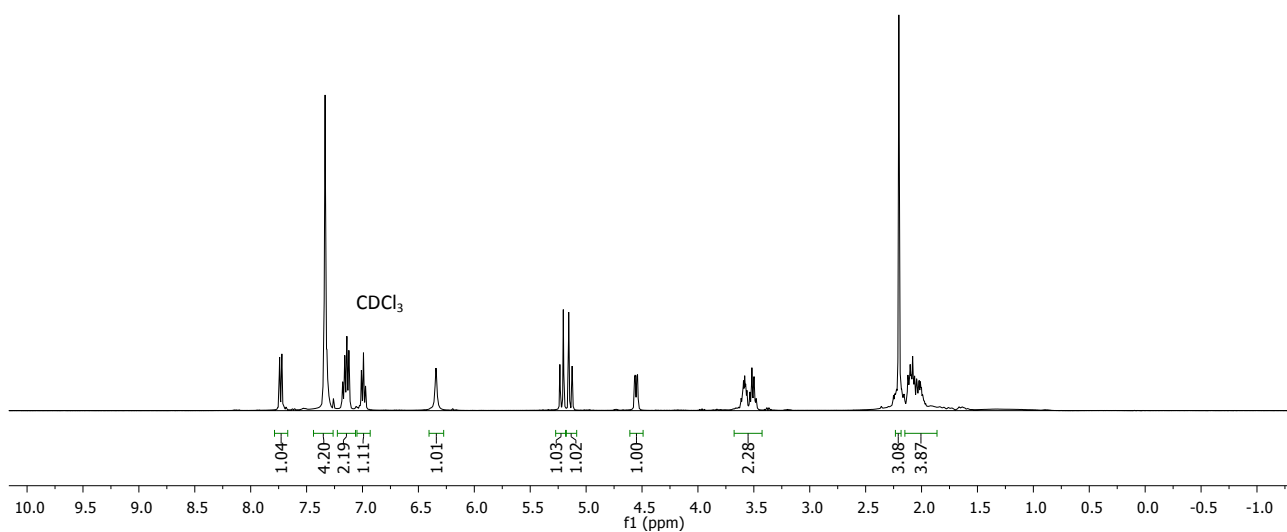
^1H NMR (400 MHz, CDCl_3)



7.74
7.72
7.33
7.32
7.16
7.14
7.12
6.99

5.24
5.20
5.16
5.12
4.57
4.56
4.55
4.54

3.59
3.58
3.57
3.56
3.54
3.52
3.50
3.48
2.16
2.12
2.10
2.09
2.08
2.06
2.04
2.02
2.01
2.00
1.99



172.6

154.1

136.7
135.5
130.1
128.4
128.2
128.0
126.5
123.7
122.4

66.8

59.3

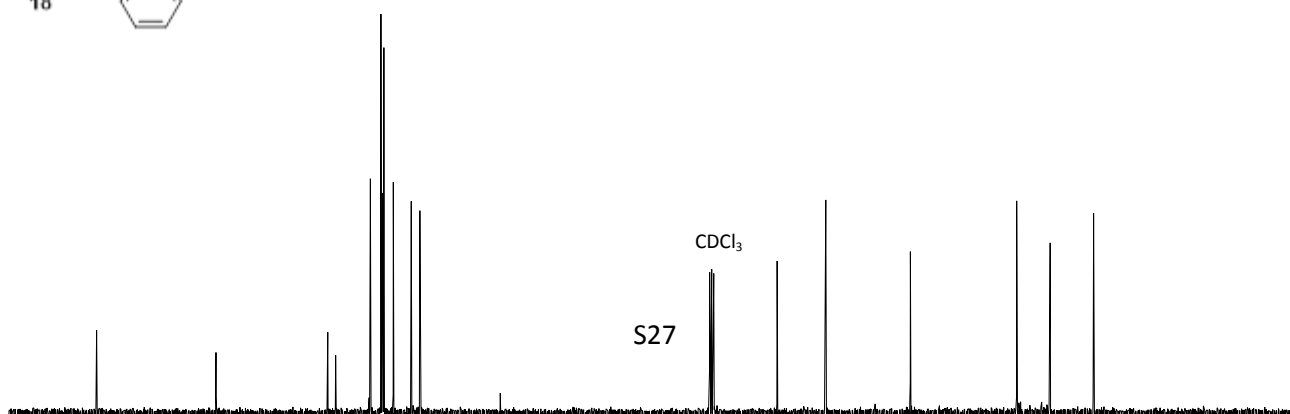
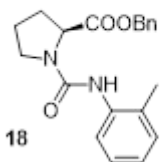
46.1

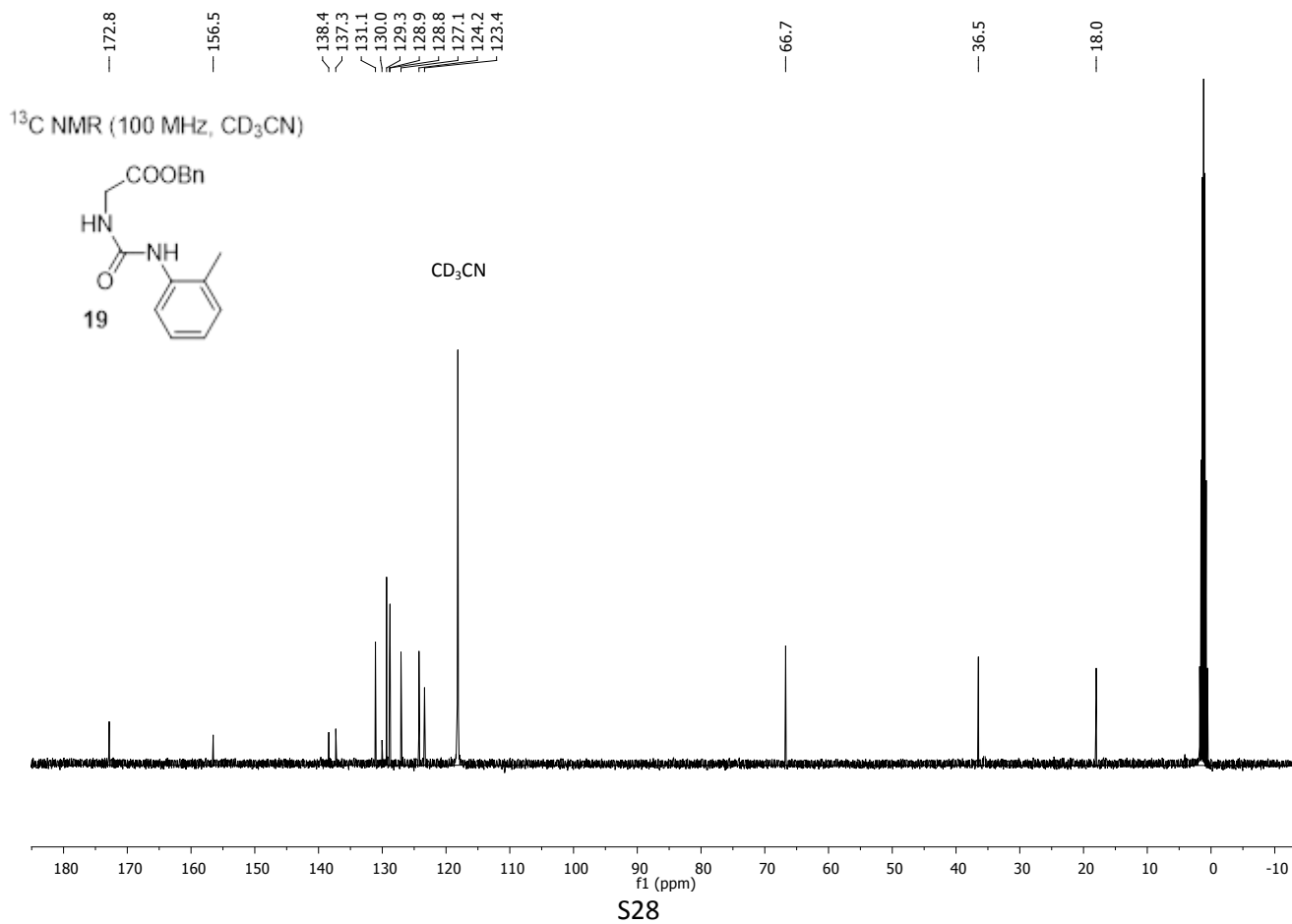
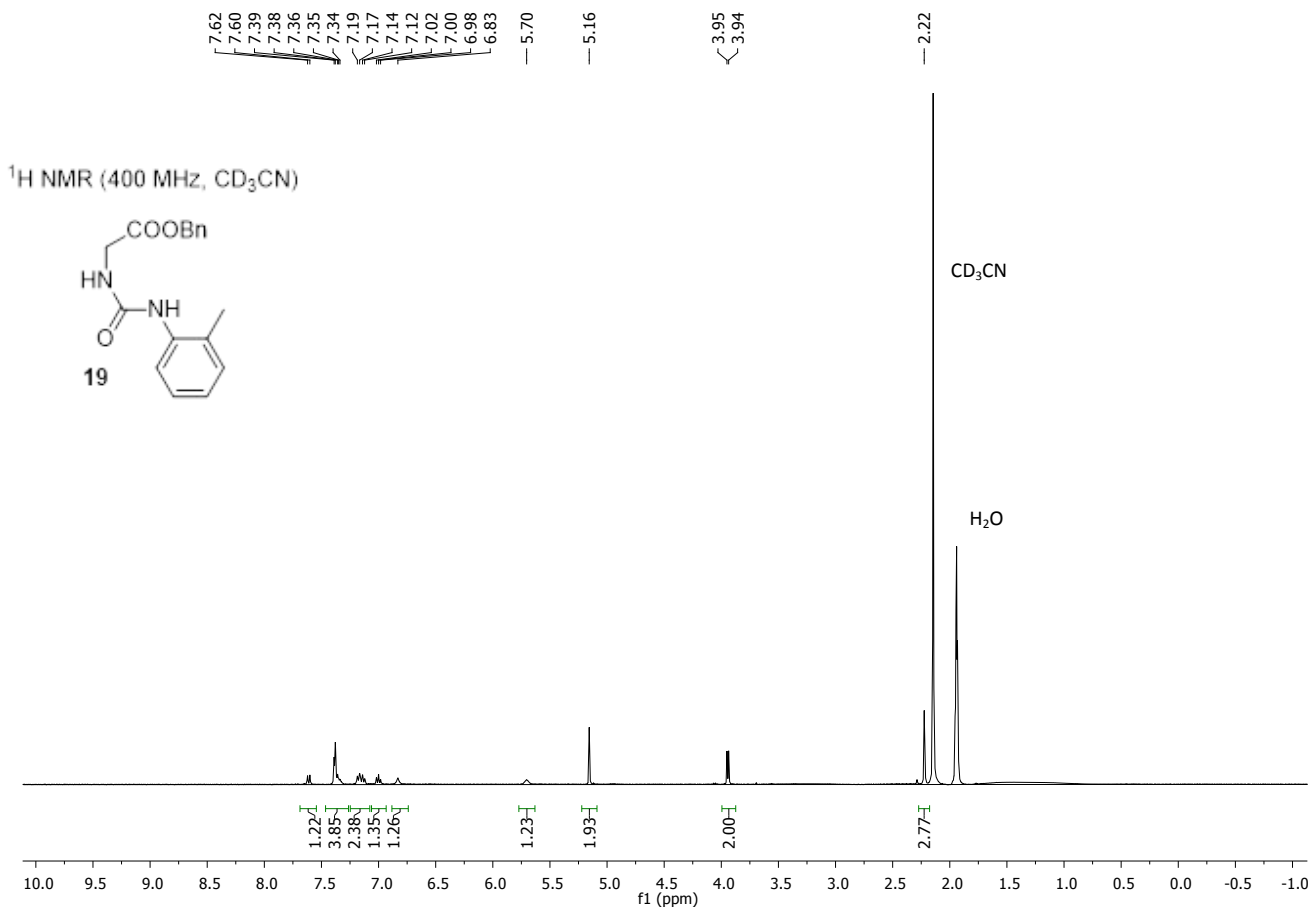
29.6

24.4

17.6

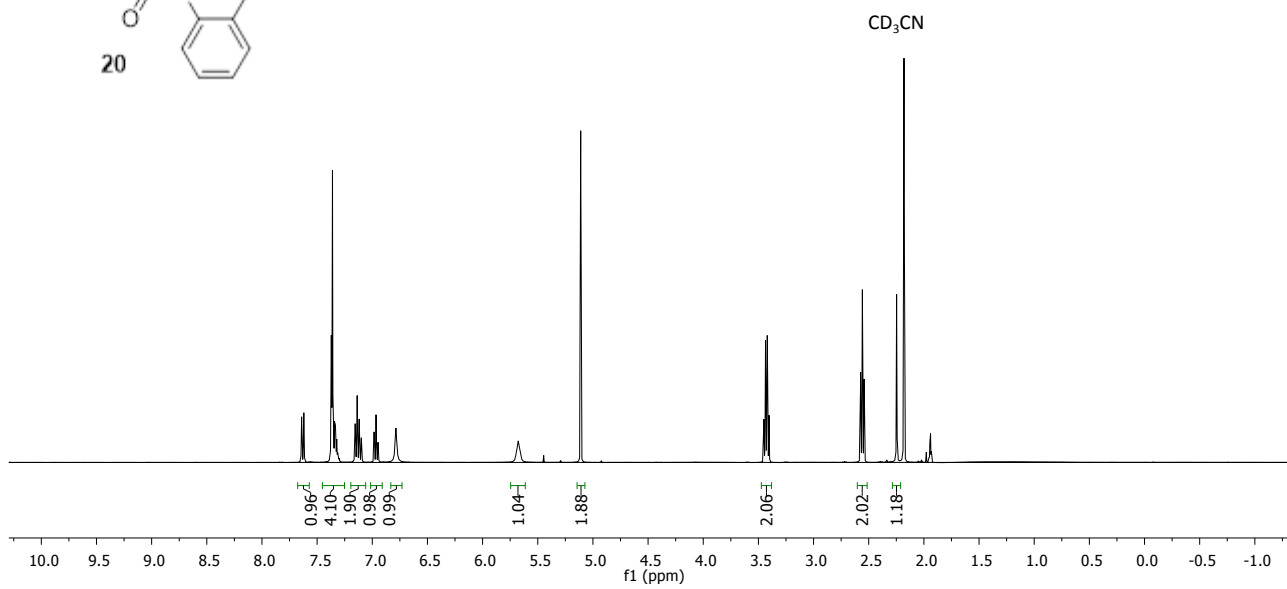
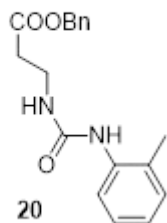
^{13}C NMR (100 MHz, CDCl_3)





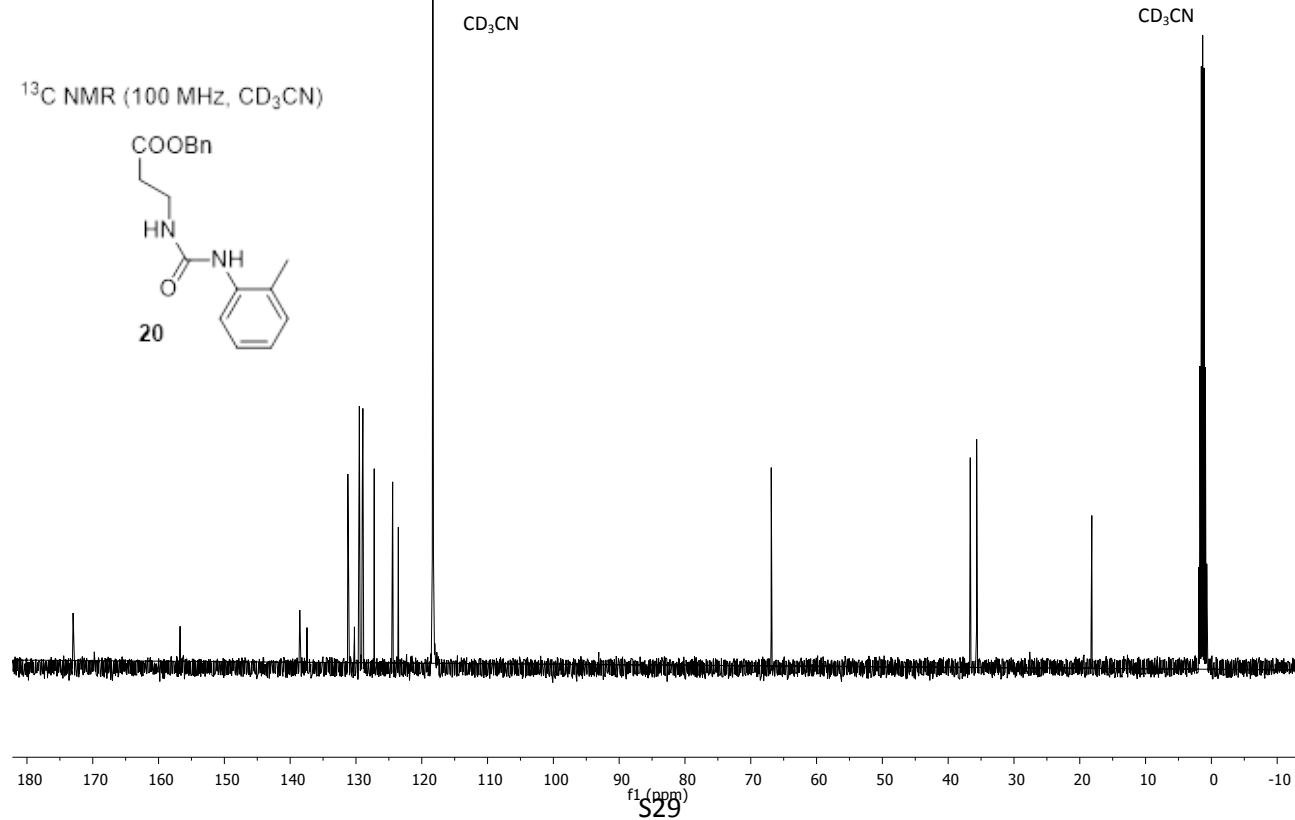
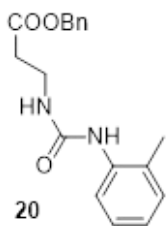
7.64
7.62
7.37
7.36
7.34
7.33
7.32
7.31
7.16
7.14
7.12
7.10
6.98
6.96
6.95
6.79
5.68
5.11
3.45
3.44
3.42
3.40
2.57
2.56
2.54
2.25

¹H NMR (400 MHz, CD₃CN)



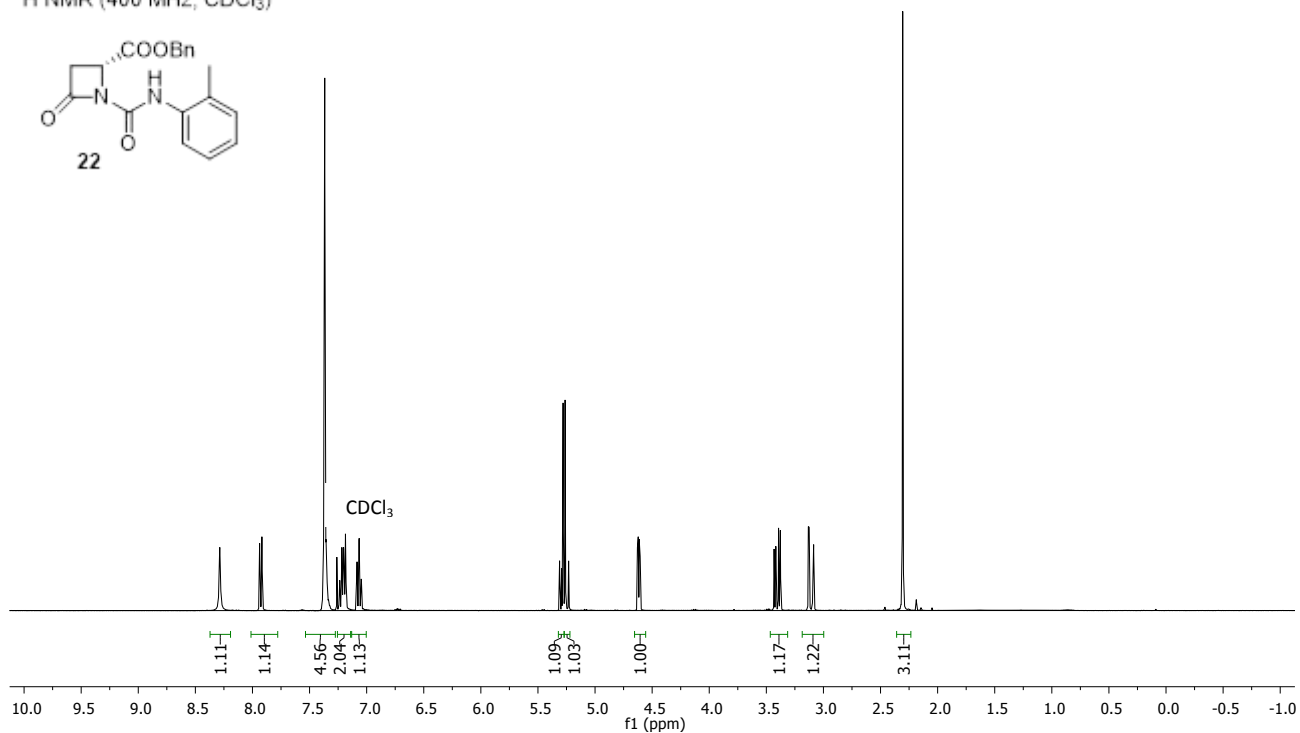
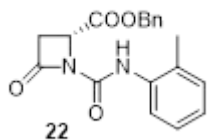
173.0
156.7
138.5
137.4
131.2
130.2
129.5
129.0
129.0
127.2
124.4
123.6
66.9
36.6
35.7
18.2

¹³C NMR (100 MHz, CD₃CN)



8.29
7.94
7.92
7.38
7.38
7.37
7.36
7.35
7.22
7.20
7.20
7.19
7.08
7.07
5.31
5.28
5.26
5.23
4.63
4.62
4.61
4.61
3.43
3.42
3.39
3.38
3.13
3.13
3.09
3.09
2.31

¹H NMR (400 MHz, CDCl₃)



168.8
165.2
146.8
135.0
134.7
130.4
128.6
128.6
128.3
127.7
126.8
124.7
121.2
67.8
48.9
41.2
17.6

¹³C NMR (100 MHz, CDCl₃)

